

AN X-RAY STRUCTURE ANALYSIS
AND SPECTRAL AND MAGNETIC STUDIES OF
SOME COMPLEX COMPOUNDS OF TITANIUM(III) WITH UNIDENTATE LIGANDS

by

Phillip H. Davis

A thesis submitted to the
University of Southampton
for the degree of
Master of Philosophy

Department of Chemistry
The University
Southampton

October 1969

ACKNOWLEDGEMENTS

It is a pleasure to take this opportunity to thank all of the individuals and organizations who have contributed to the success of this work. In particular, thanks are due to the University of Southampton, and especially the Department of Chemistry, for the provision of research facilities and to the Atlas Computer Laboratory for the use of their computing facilities and the X-RAY 63 system of X-ray crystallographic programs. I am indebted to the United States government and the United States-United Kingdom Educational Commission for the award of a study and maintenance grant under the Fulbright-Hays Act. Special thanks are due to my supervisor, Dr. J. S. Wood, whose guidance and encouragement have been central to the success of this work. Finally, thanks go to my wife, without whose patience, understanding, and encouragement this work would not have been completed.

Phillip H. Davis

ABSTRACT

FACULTY OF SCIENCE

CHEMISTRY

Master of Philosophy

AN X-RAY STRUCTURE ANALYSIS AND SPECTROSCOPIC AND MAGNETIC STUDIES
OF SOME COMPLEX COMPOUNDS OF TITANIUM(III) WITH UNIDENTATE LIGANDS

By Phillip Howard Davis

The crystal and molecular structure of hexaureatitanium(III) iodide, $[\text{Ti}(\text{CO}(\text{NH}_2)_2)_6]\text{I}_3$ has been determined from a complete set of counter collected, three-dimensional x-ray diffraction intensity data.

Refinement by conventional Fourier and least squares techniques was to a final residual of 0.064. The complex crystallizes in the space group $R\bar{3}c$ with $a = 17.67\text{\AA}$, $c = 14.15\text{\AA}$, and six formula units in the unit cell ($\rho_{\text{obs}} = 2.06$, $\rho_{\text{calc}} = 2.03 \text{ g/cm}^3$). The titanium atom occupies a special position of D_3 symmetry and is surrounded by six oxygen atoms at the vertices of a slightly distorted octahedron, the three ligand molecules above the plane of the titanium being rotated through an angle of 5.55° with respect to the three below the plane. The iodide ions form essentially linear chains parallel to the crystallographic three-fold axis.

Ligand field calculations based on the molecular structure so determined have been used to interpret the spectral and magnetic properties of the complex. It has been found that for the form of trigonal distortion observed in hexaureatitanium(III) iodide, all ligand field splittings can be expressed in terms of the single parameter Dq . The ligand field calculations indicate an orbital singlet (2A_1) ground term and the recently published single crystal

spectrum polarizations have been re-examined in this light. The theoretical, principal and average magnetic moments have been calculated and compared with experimental results over the temperature range 300-100°K, taking as parameters of the system the spin-orbit coupling constant λ , Stevens' orbital reduction factor k , and Δ the splitting of the cubic field ${}^2T_{2g}$ term in the trigonal field. The complete set of trigonal-field wave functions has been used as a basis set and mixing of the upper excited 2E level with the ground terms under spin-orbit coupling was considered. A high degree of reduction in λ and k as well as possibly significant second-nearest neighbor effects are indicated.

Attempts to prepare an analogous complex of thiourea have been unsuccessful, although definite evidence for the existence of a complex of titanium(III) with thiourea has been obtained.

CONTENTS

	Page
CHAPTER 1 Chemical Background	1
CHAPTER 2 Introduction to the X-Ray Structure Determination	10
CHAPTER 3 Elements of Ligand Field Theory and Its Application to Spectral and Magnetic Properties of Complexes	20
CHAPTER 4 Preliminary X-Ray Work	30
CHAPTER 5 X-Ray Structure Determination and Refinement	35
CHAPTER 6 Interpretation of Spectral and Magnetic Properties	53
CHAPTER 7 Attempted Preparation of a Complex of Titanium(III) with Thiourea	69
APPENDIX A Observed and Calculated Structure Factors	74
APPENDIX B Least Squares Weighting Scheme for Counter Collected X-Ray Diffraction Intensity Data	75
APPENDIX C Anisotropic Temperature Factor Relations for Atoms on Special Positions	78
APPENDIX D Summary of Matrix Elements Used in Magnetic Moment Calculations.	81
References	86

CHAPTER 1

CHEMICAL BACKGROUND

The electronic spectra of complexes of trivalent titanium were among the first to be assigned on the basis of crystal field theory. In the early 1950's, Hartmann and co-workers¹⁻⁴ identified the weak absorption in the visible region of the electronic spectrum of the $[\text{Ti}(\text{H}_2\text{O})_6]^{3+}$ ion and several other six-coordinate titanium(III) species as arising from the transition of the single d-electron between the ${}^2\text{E}_g$ and ${}^2\text{T}_{2g}$ terms which result from the splitting, by an essentially cubic crystal field, of the originally five-fold degenerate ${}^2\text{D}$ ground term of the free ion. Since that time the study of complexes of trivalent titanium has been closely linked to developments in concepts of structure and bonding in transition metal complexes.

Because such systems contain but a single d-electron, the electronic spectra and magnetic properties of complexes of titanium (III) should potentially be among the simplest to interpret on the basis of theory, and it might be expected that they would be among the most widely studied. That this is not so is probably due largely to the difficulty in preparing and handling these compounds which readily undergo hydrolysis and oxidation. Improvements in techniques for the handling of air and moisture sensitive compounds have somewhat alleviated such difficulties, and these developments, coupled with theoretical advances, have prompted a renewed interest in the complex chemistry of titanium(III). Recent re-examination of some of the earlier studies has shown them to have been in error, and, as exact structural information becomes available, further re-interpretations can be expected.

(i) Ionic complexes of titanium(III) with oxygen donor ligands.

Titanium(III) forms ionic complexes with a number of oxygen donor ligands, notably water, various alcohols, and urea.

The existence of the $[\text{Ti}(\text{H}_2\text{O})_6]^{3+}$ unit in the cesium alum, $\text{CsTi}(\text{SO}_4)_2 \cdot 12\text{H}_2\text{O}$, has been established by X-ray structure analysis.^{5,6} Hartmann and co-workers^{1,2} showed that this species was also common to aqueous and dilute HCl and H_2SO_4 solutions of titanium(III). Using calculations based on crystal field theory they were able to assign the weak ($\epsilon_{\text{mol}} \sim 4$) absorption at about 20300 cm^{-1} in the crystal spectrum of the alum and the spectra of the solutions to the transition of the single d-electron between the ${}^2\text{E}_g$ and ${}^2\text{T}_{2g}$ terms produced by the action of the crystalline field of the six water dipoles on the energy levels of the free ion. These same authors also studied the spectra of solutions of titanium(III) in various alcohols^{3,4} and in water and alcohol containing urea.⁴ On the basis of the similarity of the spectra to that of the $[\text{Ti}(\text{H}_2\text{O})_6]^{3+}$ ion (cf. Table 1.1) they formulated the absorbing species in each case as involving titanium octahedrally coordinated to six equivalent ligands. The absorption band for the hexaquo ion was asymmetrical with a slight shoulder on the high wave-length side, while the spectra of the alcohol and urea complexes exhibited two distinct maxima. Both effects have been attributed to the lowering of the symmetry of the coordination polyhedron from regular octahedral or to the action of a dynamic Jahn-Teller effect.⁷

The crystalline hexahydrates $\text{TiCl}_3 \cdot 6\text{H}_2\text{O}$ and $\text{TiBr}_3 \cdot 6\text{H}_2\text{O}$ may be precipitated by passing HCl or HBr gas through cold, aqueous solutions of the corresponding titanium trihalide.^{8,9} In contrast to the spectra of aqueous solutions of TiCl_3 and TiBr_3 with their single

TABLE 1.1
ELECTRONIC SPECTRA OF SOME COMPLEXES OF
TITANIUM(III) WITH WATER, ALCOHOLS, AND UREA

SYSTEM	BAND MAXIMA (CM ⁻¹)	ε	REF.
CsTi(SO ₄) ₂ · 12H ₂ O	20,300*	4.1	1
TiCl ₃ · H ₂ O	20,300	4.1	1
TiCl ₃ · 0.1N HCl	20,000	4.0	3
Ti ₂ (SO ₄) ₃ · 0.1N H ₂ SO ₄			
TiCl ₃ · CH ₃ OH	15,000-16,600	3.8, 4.2	3
TiCl ₃ · C ₂ H ₆ OH	15,000-16,500	3.4, 3.8	3
TiCl ₃ · CO(NH ₂) ₂ · CH ₃ OH	16,000-17,500	10.6, 10.6	4
TiCl ₃ · CO(NH ₂) ₂ · H ₂ O	16,250-18,000	10.1, 11.5	4
[Ti(CO(NH ₂) ₂) ₆] ₃ I ₃	16,530-18,200*		4
	16,300-18,100**		4

* Crystal spectrum

** Diffuse reflectance spectrum

asymmetric absorption band in the visible region, the reflectance spectra of the crystalline hexahydrates are characterized by a well resolved doublet (maxima at 18300 and 15000 cm⁻¹ for the chloride and 18500 and 13900 cm⁻¹ for the bromide). A recent study by Schlafer and Fritz¹⁰ of the far infrared spectra of these compounds has produced evidence for metal-halogen bonding and the formulation [Ti(H₂O)₄X₂]_x · 2H₂O has been suggested rather than one

involving the hexaquo ion as previously supposed.

Increasing the chloride content (e.g. by addition of chloride salts or passage of HCl gas) of aqueous solutions of TiCl_3 results in a shift of the absorption maximum from about 20000 cm^{-1} to about 14500 cm^{-1} , presumably accompanying substitution of Cl^- for H_2O in the first coordination sphere of the titanium. H. J. Gardner¹¹ has studied the formation constants of the expected series of chloro-aquo ions $[\text{Ti}(\text{H}_2\text{O})_{6-n}\text{Cl}_n]^{3-n}$. His results indicate that a major species in concentrated HCl solutions of TiCl_3 , such as those from which the hexa-hydrate is precipitated, should indeed be $[\text{Ti}(\text{H}_2\text{O})_4\text{Cl}_2]^+$.

Hartmann and Schlafer have precipitated a green solid by passing HCl gas through an aqueous solution of TiCl_3 covered with a layer of ether; however, attempts to isolate the solid produced only the violet hexahydrate. Solid compounds $\text{M}_2\text{TiCl}_5 \cdot \text{H}_2\text{O}$ ($\text{M} = \text{Cs}, \text{Rb}$) have been prepared by Stahler.^{8,12} It has been suggested that these probably involve octahedrally coordinated titanium(III) with the sixth position being occupied by the water molecule, but structural data is completely lacking. In the presence of even small traces of the F^- ion, aqueous titanium(III) solutions take on a green coloration, but little or no work seems to have been done on the composition of the probable fluoro-aquo complex involved.

By analogy with the corresponding vanadium(III) complexes and on the basis of the position of the absorption maximum at 16800 cm^{-1} Clark¹³ argues that the absorbing species in the alcoholic solutions should more probably be formulated as $[\text{Ti}(\text{ROH})_4\text{X}_2]^+$. The latter evidence would seem to be of dubious value as a priori calculations based on present theory are at best semi-quantitative. Schlafer and

Gotz,¹⁴ however, have prepared the two series of compounds $\text{TiCl}_3 \cdot 4\text{ROH}$ (blue in colour) and $\text{TiBr}_3 \cdot 4\text{ROH}$ (green in colour) with the alcohols i-propanol, s-butanol, and cyclohexanol. The reflectance spectrum in each instance is identical to the solution spectrum of the complex in the parent alcohol, and, as the energy of the ${}^2\text{E}_g \leftarrow {}^2\text{T}_{2g}$ transition is inconsistent with tetrahedral coordination of the titanium, they have concluded that the absorbing species in each case is the $[\text{Ti}(\text{ROH})_4\text{X}_2]^+$ unit. Hartmann and Schlafer¹ report another chloro-alcoholato complex formed by dissolving titanium metal in absolute ethanol with the introduction of HCl gas. A green solution results, but it was not possible to obtain a solid.

The hexahalo ions TiF_6^{3-} , TiCl_6^{3-} and TiBr_6^{3-} are known, as well as a few instances of ionic complexes involving nitrogen donor ligands, but the only examples of complexes of titanium(III) involving the titanium-sulfur bond appear to be the neutral adduct molecules $\text{TiX}_3 \cdot 2\text{L}$ where $\text{X} = \text{Cl}^-$, Br^- , or I^- and $\text{L} =$ tetrahydrothiophen and dimethyl sulfide.¹⁵

A comprehensive review of the complex chemistry of titanium(III) may be found in the recent monograph by Clark¹³ (especially Chapters 4 and 6).

(ii) Complexes involving the $[\text{Ti}(\text{urea})_6]^{3+}$ ion.

A compound containing the hexaureatitanium(III) ion was first reported by Barbieri¹⁶ who isolated the perchlorate salt. This salt, however, is not particularly well suited to studies of the complex in the solid state, being extremely hygroscopic and oxidising readily in moist air. Hartmann et.al.⁴ have prepared the iodide salt according to the following procedure:

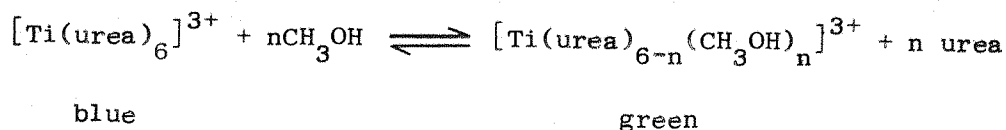
4 g TiCl_3 are added with stirring to an ice-cold solution of 25 g urea in 25 ml water. The resultant dark blue solution is filtered to remove impurities and any undissolved urea and a hot solution of 50 g KI in 30 ml added. Upon cooling, the complex crystallizes out as dark blue, hexagonal needles.

The size of the crystals can be controlled over a wide range by regulating the rate of cooling. This salt is not hygroscopic and, in contrast to most complexes of titanium(III), is relatively stable toward oxidation in dry air.

It has been suggested that the unusual stability of the iodide salt of the hexaurea complex arises from hydrogen bonding, either of an intramolecular nature among the coordinated urea molecules, or between cation and ion. Clark and Greenfield¹⁷ have prepared a series of complexes of substituted ureas to determine the effect on the stability of the complex of replacing the amino-hydrogens. N-methylurea gave a complex of the type $[\text{TiL}_6]^{3+}$ comparable in stability to the urea complex, but dimethylurea (both symmetrical and asymmetrical) and tetramethylurea both gave only complexes of the form $\text{TiCl}_3 \cdot 3\text{L}$ of much lower stability. The change in stoichiometry was attributed to the combination of steric factors and inductive effects contributing to the different donor abilities of the oxygen atoms in the substituted ureas. O'Donnell and Davis¹⁸ have isolated a complex with tetrahydro-2-pyrimidone ($\text{C} \begin{array}{c} \diagup \text{C}-\text{N} \diagdown \\ \diagdown \text{C}-\text{N} \diagup \end{array} \text{C} = \text{O}$) using a procedure analogous to that employed in the preparation of the iodide salt of the urea complex. On the basis of absorption and reflectance spectra, it appears to involve a $[\text{TiL}_6]^{3+}$ type ion, although the stability is again much less than that of the urea complex.

If a concentrated solution of hexaureatitanium(III) iodide in methanol is diluted with a small amount of methanol, the colour of the solution undergoes a change from blue to green,⁴ presumably

accompanying a partial replacement of coordinated urea by alcohol



The change is reversible, and if the solution is saturated with urea, the blue coloration returns. Successive dilutions of an aqueous solution result in a shift of the absorption maxima to higher wave-numbers. However, even at the highest dilutions studied it remains shifted approximately 1000 cm^{-1} to the red with respect to the absorption of the hexaquo ion. This has been interpreted as an indication that one or more urea molecules remain bound in the inner coordination sphere.

Coordination of the urea molecules through the oxygen atoms has been inferred from the downward shift of the carbonyl stretching frequency compared with its value in the free ligand.¹⁹ This conclusion has been confirmed by the X-ray structure determination of Linek and co-workers²⁰ who have solved the structure of the salt in projection along the c axis. (The c crystallographic axis is parallel to the needle axis of the crystal). The compound crystallizes in the space group $R\bar{3}c$ with $a = 17.72$ and $c = 14.26 \text{ \AA}$ and six formula units in the unit cell. The titanium atoms are located on special positions of D_3 symmetry and in a plane with three iodide ions. The oxygen atoms are reported to lie at the corners of a regular octahedron, the urea molecule being oriented with one amide grouping directed toward the iodide ions. The Ti-O-C bond angle is approximately 120° .

From the similarity, both in the position and the intensity of the absorption, of the spectra of solutions of titanium(III) in both

urea-saturated water and urea-saturated methanol, as well as the crystal and reflectance spectra of the hexaureatitanium(III) iodide salt, it has been concluded that the $[\text{Ti}(\text{urea})_6]^{3+}$ ion is the absorbing species in each instance. The absorption consists of a single broad band centred at about 17000 cm^{-1} with two distinct maxima, the splitting between the two maxima amounting to about 2500 cm^{-1} (cf. Table 1.1). The splitting of the absorption band has been attributed to the action of a dynamic Jahn-Teller effect on the excited e_g^* state.⁷ Van Vleck²¹ has shown that the magnitude of any Jahn-Teller splitting of the ground state (t_{2g}) would be much less than that observed. The temperature dependence of the splitting in the crystal spectra measured by Dingle²² is also consistent with an excited state origin for the splitting.

The site symmetry of the Ti^{3+} ion is D_3 . Within this framework the ${}^2T_{2g}$ ground term of the octahedral model can be decomposed into an orbital singlet (2A_1) and an orbital doublet (2E). On the basis of the polarization of the crystal spectrum, Dingle²² assigns the 2E as the ground term. The absorption has both a π and a σ intensity* but the π intensity, particularly of the lower energy component, is much greater. Within the model used, transitions from an 2A_1 ground state would be σ polarized only. Since the σ and axial spectra coincide, the transition must be electric dipole or electric quadrupole in nature.

* In the orthoaxial spectra of a uniaxial crystal the light may be polarized with the electric vector either parallel to the optical axis \underline{c} or perpendicular to \underline{c} . The former case is designated as the π spectrum and the latter as the σ spectrum.

The room temperature magnetic moments of both the perchlorate^{23,27} and iodide^{4,25} salts are close to the spin only value of 1.73 B.N. The susceptibilities of these two compounds have been measured over the range 300-80°K. The results have been analyzed by the method of Figgis²⁶⁻²⁸ to yield estimates of the splitting of the ground state (Δ), the spin-orbit coupling constant (λ), and Steven's orbital reduction parameter (k).^(a) For both salts,²³⁻²⁵ Δ has been found to be about 450 cm⁻¹ with the orbital singlet state (2A_1) lying lowest, in conflict with the assignment based on the polarization of the crystal spectrum.

(iii) Purpose of the present study.

The present work has as its main purpose the determination of a refined crystal and molecular structure for hexaureatitanium(III) iodide based on a complete set of three dimensional X-ray data.

The implications for the spectral and magnetic properties of the complex of the structure so determined will be investigated. In particular, an attempt will be made to correlate the anisotropies of these properties with the deviation of the ligand field from octahedral symmetry.

The preparation and characterization of the analogous thiourea complex will also be attempted.

(a) The parameter $k(\leq 1)$ is the amount by which the orbital angular momentum part of the magnetic moment operator $[(L + 2S)\beta]$ is reduced on complex formation. It has been associated with delocalisation of the unpaired electron(s) into ligand orbitals and as such has been taken as a measure of covalency. Gerloch²⁹ has recently reviewed the significance of k in magnetochemistry.

CHAPTER 2

INTRODUCTION TO THE X-RAY STRUCTURE DETERMINATION

A crystal may be considered as a three-dimensional array of identical subunits (the unit cell) which gives rise to a continuous, periodic electron density function. The translations by which the repeat units of the array are related are of the same order of magnitude as the wave lengths of x-rays, and consequently the interaction of x-rays with the resultant electron density gives rise to diffraction. A consideration of the geometry of the phenomenon of diffraction will show that x-rays scattered from different points in successive planes of the lattice array will be in phase and give a resultant beam of maximum intensity if and only if the angle between the normal to that incident beam and the normal to the scattering planes is such that

$$n\lambda = 2d\sin\theta \quad n = 0, 1, 2 \dots \quad (1)$$

where θ is the angle defined above, d the interplanar spacing, and λ the wave length of the incident radiation. This is Bragg's law.

As a result of the above relation it is possible to deduce, from a study of the directions in space of the intensity maxima in the diffracted beam, information about the distances which relate the sub-units of the array, that is, about the dimensions and shape of the unit cell.

While the directions of the maxima are dependent only on the size of the unit cell, their absolute magnitudes depend on the arrangement of the electron density, i.e. the atoms, within the

unit cell. Since x-rays are scattered by electrons, the scattering power of an isolated atom is related to its atomic number. In practice, the electron cloud about an atom is of finite size and x-rays scattered from various points within it will be slightly out of phase, resulting in a scattering factor (designated f_j) which is a decreasing function of $\sin\theta/\lambda$. The scattering power of the entire contents of the unit cell is defined in terms of a quantity known as the structure factor, F_{hkl} , which may be considered as the resultant of j waves scattered in the direction of the hkl reflection by the j atoms of the unit cell. The waves are vector quantities and application of the laws of vector addition gives rise to the following two equivalent expressions for F_{hkl} :

$$F_{hkl} = (A_{hkl}^2 + B_{hkl}^2)^{1/2}, \quad \alpha = \tan^{-1} \left(\frac{B_{hkl}}{A_{hkl}} \right) \quad (2a)$$

where α is the phase angle and where

$$A_{hkl} = \left[\sum_j f_j \cos 2\pi(hx_j + ky_j + lz_j) \right]$$

$$B_{hkl} = \left[\sum_j f_j \sin 2\pi(hx_j + ky_j + lz_j) \right]$$

or

$$F_{hkl} = \sum_j f_j e^{2\pi i(hx_j + ky_j + lz_j)} \quad (2b)$$

It is worthwhile noting that for centrosymmetric structures B in (2a) above is zero. This is computationally convenient, but more importantly, it means that the phase angle α must be either 0 or π (i.e. The structure factors are real numbers with phases of either + or -). This fact has important consequences for the applicability

of the heavy atom approach to the phase problem.

Detailed discussions of the theory of x-ray diffraction by crystals are available in a number of standard texts.³⁰⁻³³

(i) Fourier methods.

Any continuous, periodic function may be represented by means of a Fourier series. Two equivalent general forms of the one-dimensional Fourier series are given below:

$$f(X) = \sum_{h=-\infty}^{\infty} c_h e^{2\pi i h x} \quad (3a)$$

$$f(X) = \sum_{h=-\infty}^{\infty} c_h (\cos(2\pi i h x) + i \sin(2\pi h x)) \quad (3b)$$

The electron density, ρ , at any point (x, y, z) in a crystal is given by

$$\rho(x, y, z) = \frac{1}{V} \sum_{hkl} \sum_{hkl} F_{hkl} e^{-2\pi i (hx + ky + lz)} \quad (4)$$

where V is the volume of the unit cell. Comparison of 3a with 4 will show that the electron density is a three-dimensional Fourier series whose coefficients, c_h , are the structure factors, F_{hkl} . Thus, if the F_{hkl} are known, it is possible to calculate $\rho(x, y, z)$ exactly. Unfortunately, the F_{hkl} are vectors possessing both a magnitude and a phase, while the crystallographic observables, the diffraction intensities, have magnitude only ($|F_{hkl}|^2$).

In the crystallographic application of the Fourier synthesis the phases calculated on the basis of some model are combined with the observed magnitudes and used to calculate a ^{trial} ~~trial~~ electron density distribution. ~~which is compared to the observed distribution.~~ (Use of both phases and magnitudes calculated from the model would, of course, result in a distribution identical to the original model). This

distribution is used ^{to derive} ~~as the basis for~~ a revised model and a new set of structure factors ^{is} λ calculated whose phases in turn are used with the observed magnitudes to calculate a revised electron density distribution. This process is repeated until the desired degree of agreement between the observed and calculated ^{structure factors} ~~distributions~~ is reached.

A variety of techniques have been employed for determining the original model to be used in phasing. If one (or a relatively small number) of the atoms in the unit cell is much heavier than the remainder, as is frequently the case in coordination compounds where the central metal ion is much heavier than the constituent atoms of the ligands, it is possible to use the so called "heavy atom" approach. The general expression for the structure factor (2b) may be rewritten

$$F_{hkl} = f_H e^{2\pi i(hx_H + ky_H + lz_H)} + \sum_n f_{Le}^{2\pi i(hx_L + ky_L + lz_L)} \quad (5)$$

If $f_H \gg f_L$, the first term of 5 dominates. In the centrosymmetric case, where all the structure factors are real, this gives rise to a particularly simple situation, for whenever the first term dominates, the sign of F_{hkl} may be taken as that given by the heavy atom. In particular, it has been shown that if the sum of the squares of the atomic numbers of the heavy atoms is approximately equal to that of the light atoms, then in a centrosymmetric structure the phases of roughly three quarters of the structure factors will be correctly determined by the heavy atoms. In the non-centrosymmetric case, where there is a continuous range of phases, the analysis is not so straightforward, but is similar in principle. A second type of Fourier

synthesis is especially useful in locating the positions of heavy atoms in the unit cell.

Patterson³⁴ has shown that a Fourier series whose coefficients are the squares of the structure factors gives information not on the electron density distribution within the unit cell, but rather on the orientation and magnitude of the interatomic vectors. Thus a peak in the Patterson function at a point (u,v,w) arises from atoms at points (x_1, y_1, z_1) and (x_2, y_2, z_2) such that

$$x_2 - x_1 = u$$

$$y_2 - y_1 = v$$

$$z_2 - z_1 = w.$$

It will be noted that for every peak at (u,v,w) in the vector space, there will be a similar peak at $(-u,-v,-w)$, that is, the Patterson function is centrosymmetric regardless of the symmetry of the unit cell. The magnitude of the peak at (u,v,w) is proportional to the product of the electron densities at (x_1, y_1, z_1) and (x_2, y_2, z_2) .

Practically, it is proportional to the product of the atomic numbers of the atoms assumed to be located at these two points. Assuming the validity of Friedel's law ($|F_{hkl}| = |F_{\bar{h}\bar{k}\bar{l}}|$)

$$P(u,v,w) = \frac{1}{V} \sum \sum \sum |F_{hkl}|^2 \cos 2\pi(hu + kv + lw) \quad (6)$$

The N atoms in the unit cell will give rise to N^2 interatomic vectors, N of which, between each atom and itself, will be located at the origin. Because the electron density about an atom is of finite size, peaks in the Patterson function will tend to be diffuse, and, if the unit cell contains a moderate number of atoms, overlapping

as well as superposition of peaks can be expected. Thus, the N^2 -N vectors not at the origin are rarely distinct. If, however, one or more atoms have a considerably higher atomic number than the majority, the peaks between these heavy atoms, and possibly those between heavy and light atoms, should stand out against the diffuse background of overlapping vectors between light atoms.

A third Fourier series of special utility in x-ray structure determinations is one whose coefficients are the differences between the amplitudes of the observed and calculated structure factors. The difference Fourier may be conceived as the difference between the observed electron density and the electron density due to the model and is closely related to the errors and inadequacies of a given model. It is particularly useful for locating the hydrogen atoms in a structure. Due to the finite size of the atomic peaks and to anomalies arising from series termination errors, hydrogen atoms in a normal Fourier synthesis rarely appear as more than "bumps" on the electron density of the atom to which they are bound. However, the presence of a hydrogen atom will give rise to an observed structure factor which is locally greater in magnitude than that calculated on the basis of a model not including the hydrogen atom. For a fairly accurate model, $|F_o| - |F_c| \approx 0$ at most points and the excess electron density due to the hydrogen atom will be emphasized.

(ii) Refinement based on the method of least squares.

Once a model has been developed which embodies reasonably accurate structural parameters, it is possible to refine these on the basis of the principle of least squares.

Consider a linear function in an n-dimensional space

$$f = a_1 x_1 + a_2 x_2 + \dots + a_n x_n \quad (7)$$

The value of f is determined both by its position in space (x_1, x_2, \dots, x_n) and by the values of the parameters a_j . If the value of f is measured at m fixed points in space, $m > n$, the best values of the a_j , in the least squares sense, are those which minimize the sum of the squares of the weighted deviations between the observed and calculated values of the function, that is, it is desired to minimize the function

$$D = \sum_{i=1}^n w_i (f_{oi} - f_{ci})^2 \quad (8)$$

Differentiation of the right hand side of (8) with respect to each of the parameters in turn and setting of the derivatives equal to zero results in a system of n linear equations in n unknowns (the a_j 's) known as the normal equations which may be expressed in the form shown below

$$\begin{aligned} \sum_{i=1}^m w_i x_{i1}^2 a_1 + \sum_{i=1}^m w_i x_{i1} x_{i2} a_2 + \dots + \sum_{i=1}^m w_i x_{i1} x_{in} a_n &= \sum_{i=1}^m w_i f_{oi} x_{i1} \\ \sum_{i=1}^m w_i x_{i2} x_{i1} a_1 + \sum_{i=1}^m w_i x_{i2}^2 a_2 + \dots + \sum_{i=1}^m w_i x_{i2} x_{in} a_n &= \sum_{i=1}^m w_i f_{oi} x_{i2} \\ \vdots & \vdots \\ \sum_{i=1}^m w_i x_{in} x_{i1} a_1 + \sum_{i=1}^m w_i x_{in} x_{i2} a_2 + \dots + \sum_{i=1}^m w_i x_{in}^2 a_n &= \sum_{i=1}^m w_i f_{oi} x_{in} \end{aligned} \quad (9)$$

Although computationally tedious, the solution of these equations, if one exists, for the best value (in the least squares sense) of the parameters a_j is straightforward.

The form of (8) suggests that a suitable function for minimization might be

$$D = \sum_{hkl} w_{hkl} (|F_{ohkl}| - |F_{chkl}|)^2 \quad (10)$$

where F_o and F_c are the observed and calculated structure factors respectively and the sum is taken over all observed reflections hkl . Unfortunately, the analytical form of the structure factor is not linear and an exact solution of the normal equations is not possible. In practice, however, the structure factor may be approximated by a Taylor series expanded about a set of approximate values, b_j , for the a_j and made linear by neglecting terms in $(a_j - b_j)$ of powers higher than the first. Thus,

$$F(a_1 a_2 \dots a_n) \sim f(b_1 b_2 \dots b_n) + \frac{\partial f(b_1 b_2 \dots b_n)}{\partial a_1} (a_1 - b_1) + \dots + \frac{\partial f(b_1 b_2 \dots b_n)}{\partial a_n} (a_n - b_n) \quad (11)$$

If equation (11) is substituted into equation (10), the method of least squares may be applied to solve for the quantities $\Delta b_j = (a_j - b_j)$ such that the values

$$b_j^* = b_j + \Delta b_j \quad (12)$$

are better approximations to the actual values of the a_j than were the

original b_j . This process is iterated until the changes in the b_j are less than a desired value at which point they are assumed equivalent to the true values of the a_j . It is essential for the convergence of the iteration that the original b_j be reasonably good approximations to the a_j .

In applying the method of least squares to the above approximation, the resultant normal equations can be expressed in matrix notation as

$$\begin{bmatrix} a_{11} & a_{12} & \dots & a_{1n} \\ a_{21} & a_{22} & \dots & a_{2n} \\ \cdot & \cdot & & \cdot \\ \cdot & \cdot & & \cdot \\ a_{n1} & a_{n2} & \dots & a_{nn} \end{bmatrix} \begin{bmatrix} x_1 \\ x_2 \\ \cdot \\ \cdot \\ x_n \end{bmatrix} = \begin{bmatrix} v_1 \\ v_2 \\ \cdot \\ \cdot \\ v_n \end{bmatrix} \quad \text{where}$$

$$a_{ij} = \sum_{hkl} w_{hkl} \frac{\partial |F_{chk1}|}{\partial a_i} \frac{\partial |F_{chk1}|}{\partial a_j}, \quad (13)$$

$$x_j = \Delta b_j, \text{ and}$$

$$v_j = \sum_{hkl} w_{hkl} (\Delta F_{hkl}) \frac{\partial |F_{chk1}|}{\partial a_j}$$

or more simply

$$\underline{Ax} = \underline{v} \quad (14)$$

A necessary and sufficient condition for equation (14) to have a solution is that the matrix \underline{A} have an inverse, in which case

$$\begin{aligned} \underline{A}^{-1} \underline{A} \underline{x} &= \underline{A}^{-1} \underline{v} \\ \underline{x} &= \underline{A}^{-1} \underline{v} \end{aligned} \quad (15)$$

It has been shown that the value of the ij^{th} element, b_{ij} , of the inverse matrix A^{-1} is a measure of the correlation between the two parameters a_i and a_j . From the diagonal elements, b_{ii} , it is possible to obtain an estimate of the standard deviation in the parameter a_i .

$$\sigma_{a_i} = \sqrt{b_{ii} (\sum_{hkl} w_{hkl} \Delta F_{hkl}^2) / (m-n)} \quad , \text{ where } m \text{ is the number of observed reflections.} \quad (16)$$

For an accurate model, if the proper weights, w_{hkl} , have been used,

$$\sum_{hkl} w_{hkl} \Delta F_{hkl}^2 / (m-n) = 1 \text{ so that } \sigma_{a_i} = \sqrt{b_{ii}}$$

CHAPTER 3

ELEMENTS OF LIGAND FIELD THEORY AND ITS APPLICATION TO SPECTRAL AND MAGNETIC PROPERTIES OF COMPLEXES

(i) Ligand field theory: General considerations.

Among the most successful theories for interpreting the spectral and magnetic properties of coordination compounds of the transition metals has been the electrostatic crystal-field theory. In this theory, as developed by Bethe³⁵ and by Schlapp and Penney,^{36,37} the ligands are considered as providing an electrostatic field which acts as a perturbing potential, removing the field-free degeneracy of the atomic orbitals of the metal ion. The interaction is considered to be entirely electrostatic in nature and electron exchange (i.e. covalent bonding) between metal ion and ligands is neglected. In the case of the transition metals, the interaction involves primarily the d-orbitals, and the manner in which this originally five-fold degenerate set is split depends on the spatial symmetry of the ligand arrangement.

Ligand field theory, as first used by Van Vleck,³⁸ is a fusion of the molecular orbital theory of Mulliken³⁹⁻⁴¹ with crystal-field theory. Molecular orbitals are formed from linear combinations of the various atomic orbitals, with the restriction that only orbitals transforming as the same irreducible representation of the molecular point group may combine. The resulting molecular orbitals are then filled in accordance with the principles of the aufbau.

Consider the case of an octahedral complex (point group O_h) in which six equivalent ligands are located equidistant from the metal ion along three mutually perpendicular axes (x,y,z). From the

standpoint of crystal-field theory, the first effect of the resultant field is to raise the mean energy of the five d-orbitals. However, two of these, d_z^2 and $d_{x^2-y^2}$ are directed along the coordinate axes and will be destabilized to a much greater extent than the remaining three, d_{xy} , d_{xz} , and d_{yz} , which lie mainly between the axes. Thus the five d-orbitals are split into an upper orbitally doubly degenerate set and a lower orbitally triply degenerate set. These are commonly designated e_g and t_{2g} respectively on the basis of their transformation properties within the O_h point group. Turning now to the ligand field approach, the transformation properties of the various atomic orbitals under the operations of the O_h point group are shown in the table accompanying figure 3.1. The ligand orbitals available for σ bonding transform as $a_{1g} + e_g + t_{1u}$. After forming linear combinations of the ligand orbitals of suitable symmetry, they are combined in the usual way with the orbitals of the central metal atom giving rise to six bonding and six antibonding molecular orbitals. Reference to figure 3.1 will show that no orbitals of appropriate symmetry exist to form σ bonds with the t_{2g} set on the metal ion and they remain as pure metal orbitals. The e_g set can, however, participate in σ bonding giving rise to a doubly degenerate σ bonding orbital (e_g) and a doubly degenerate σ antibonding orbital set (e_g^*). If the ligand orbitals are more stable than those on the metal ion, the e_g^* set will be mainly metal in character. Thus it can be seen that in the absence of secondary effects (e.g. π -bonding), crystal field theory and ligand field theory led to qualitatively similar results. Where the ligand field potential is the primary perturbation and where only qualitative results are desired, the simpler assumptions of crystal field theory

FIGURE 3.1

MOLECULAR ORBITAL ENERGY LEVELS FOR AN OCTAHEDRAL COMPLEX

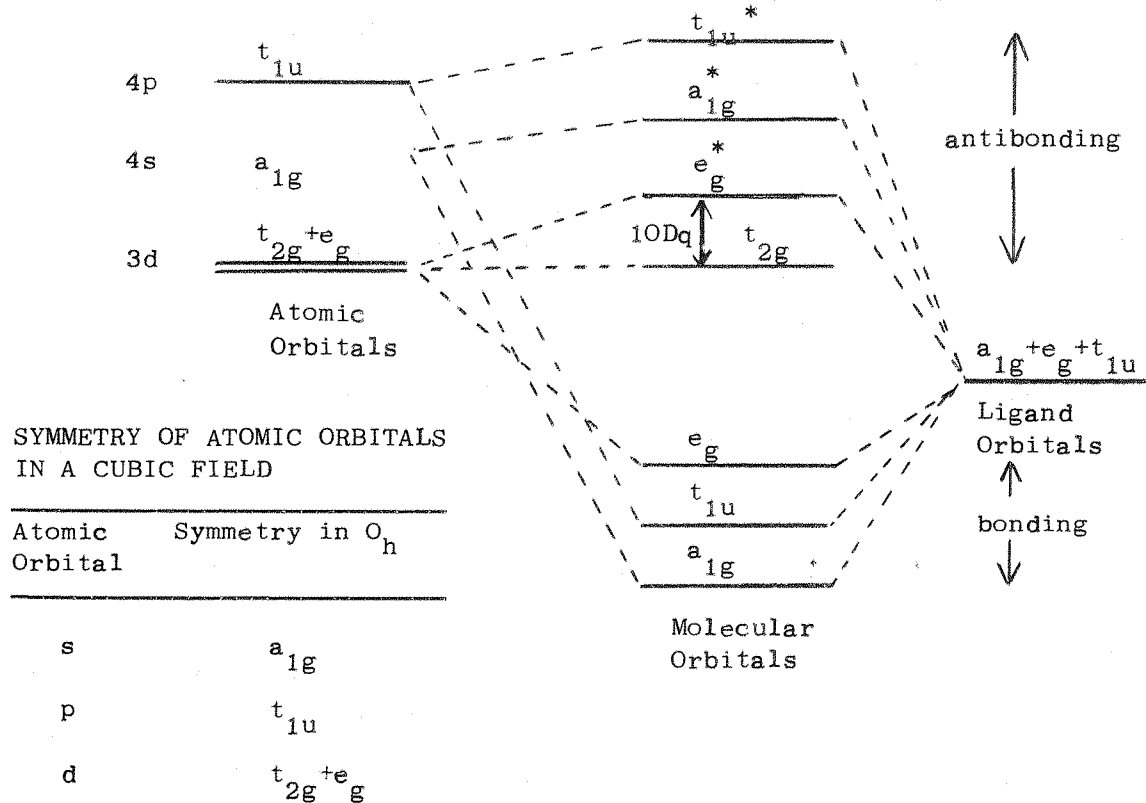
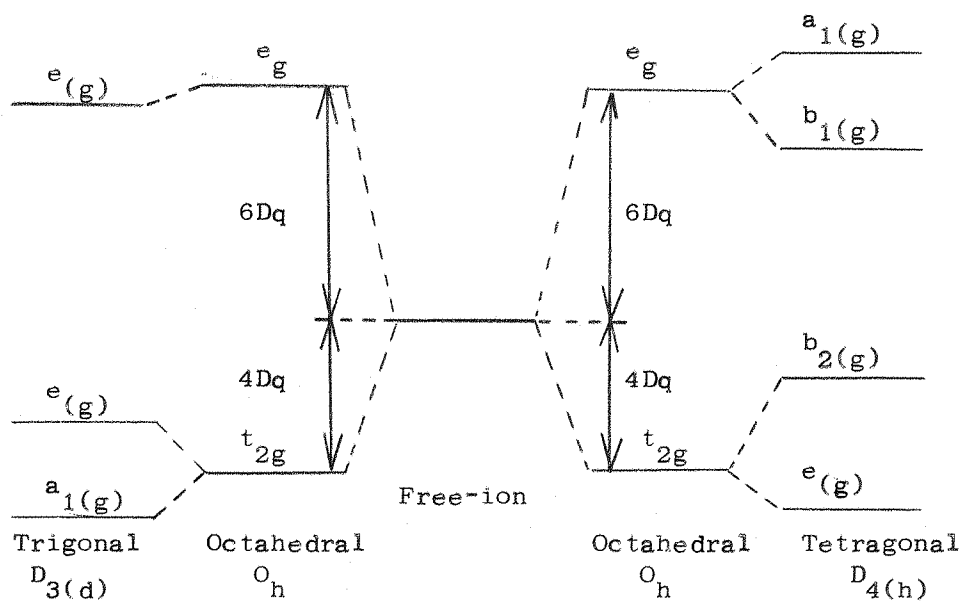


FIGURE 3.2

LIGAND FIELD SPLITTINGS FOR COMMONLY ENCOUNTERED SYMMETRIES



make it easier to work with, but where quantitative answers are required or bonding effects significant, the more complete treatment of ligand field theory is needed.

The presence of fields of symmetry lower than octahedral can further lift the remaining degeneracy of the metal orbitals. Splittings produced by symmetries commonly encountered in complexes of coordination number six are shown in figure 3.2. If the octahedron is distorted so that one of the four-fold rotation axes is maintained (point group D_4), the e_g level of the octahedral complex is split into two orbital singlets (a_1 and b_1) while the t_{2g} level decomposes to an orbital doublet (e) and an orbital singlet (b_2). The exact ordering of the levels is dependent on the sense and the magnitude of the distortion. A second commonly encountered distortion is one which maintains a three-fold axis (point group D_3). Such a trigonal distortion could be one of two types. The first, which is most commonly invoked, involves compression or elongation along the three-fold axis, resulting in a coordination polyhedron which is a trigonal antiprism. The second involves rotation of one set of three ligands with respect to the other about the three-fold axis. Carried to its extreme, such distortion would give rise to a trigonal prism.

(ii) Application to spectra.

In the majority of cases the absorption of electromagnetic radiation takes place via an electric dipole process. In such cases the intensity of the absorption is given by

$$I \propto \int \psi^* \mu(x,y,z) \psi d\tau \quad (1)$$

where μ is an operator corresponding to the vector sum of the three classical components of an electric dipole (Similar expressions hold for other types of interaction, e.g. magnetic dipole, or electric quadrupole, but the form of the operator will differ). The exact value of I can be determined only by substituting explicitly for the wave functions ψ^* and ψ and evaluating the integral, but group theoretical considerations alone can show whether it is possible for I to have a finite value.

The condition for I to be non-zero is that the direct product representation of $\psi^* \mu(x,y,z) \psi$ span the totally symmetric representation. The operator μ has the same transformation properties as the individual coordinates, in particular, it is odd (antisymmetric) with respect to inversion through a center of symmetry. From this it follows immediately that if ψ^* and ψ are either both even or both odd, the integral in (1) will be identically zero, since the product of two even and one odd, or three odd functions must be odd. This is the basis of the Laporte selection rule that transitions between states of the same parity are forbidden. If ψ^* and ψ represent states arising from a d^n configuration under the influence of a centrosymmetric field, they will possess the even character inherent in the d-orbitals, and thus transitions between them should be forbidden. Although of low intensity, absorptions corresponding to such transitions are observed and it is necessary to consider mechanisms by which they can gain a finite intensity.

In general this finite intensity is attributed either to the presence of a non-centrosymmetric component in the ligand field or

to vibronic coupling. In the former case it is thought that mixing in of the p-orbitals with the d-orbitals occurs causing the latter to lose their rigorous even character thus making the transition allowed. The case of vibronic coupling corresponds to the breakdown of the Born-Oppenheimer approximation. It is no longer possible to rigorously separate the wave function into an electronic and a vibrational part and it becomes necessary to consider integrals of the form

$$I_{ij} = \int (\psi_e' \psi_v') u(x, y, z) (\psi_e \psi_v) d\tau \quad (2)$$

where ψ_e and ψ_v represents the electronic and vibrational portions of the wave functions respectively. If the transition is assumed to take place from the vibrational ground state, ψ_v will be totally symmetric and it can be shown that, in general, I will be non-zero if $\psi_e' \psi_v$ belongs to a representation spanned by the direct product representation of $\psi_e' \mu \psi_e$.

The electric dipole operator μ corresponds to a sum and it is possible to write expressions similar to (1) and (2) for each of the coordinates x , y , and z . In environments of symmetry lower than octahedral, it may happen that x , y , and z do not all belong to the same representation. This can give rise to the phenomenon of polarization in which the transition is allowed in one or two of these directions, but not all three.

Theoretically a study of the polarization of the absorptions of a single crystal would provide a powerful tool for determining the effective symmetry of the environment of the metal ion. In practice, particularly where the intensity giving mechanism involves vibronic coupling, it is found that all transitions are allowed

(though perhaps to different extents) in spite of the inequivalence of the axes and the results of polarization studies are ambiguous.

(iii) Application to magnetic properties.

While consideration of the ligand field potential alone is sufficient to account for the basic features of the absorption spectra of transition metal complexes, interpretation of their magnetic properties requires account to be taken of the influence of spin-orbit coupling and the Zeeman effect. For the first row transition elements both of these effects are small in comparison to the ligand field splitting which allows them to be treated according to the methods of perturbation theory as a small addition to the ligand field potential. Details of the relevant calculations may be found in Appendix D and we shall be concerned presently only with the general nature of the effects.

Although small for $(3d)^n$ systems, spin-orbit coupling has important consequences for their magnetic properties, being manifest chiefly in the deviation of their measured magnetic moments from the value given by the spin-only formula

$$\mu = [4S(S + 1)]^{\frac{1}{2}} \quad (3)$$

and in the zero-field splitting. For the lighter transition elements, the existence of Russell-Saunders coupling is usually assumed. In such a case the magnetic moment is predicted to be

$$\mu = [4S(S + 1) + L(L + 1)]^{\frac{1}{2}} \quad (4)$$

For most of the early transition elements, however, the measured moments correspond fairly closely to the values predicted by (3), indicating that the orbital contribution to (4) has been effectively

quenched. This is due primarily to the ligand field. The presence of the ligand field has the effect of uncoupling the L and S vectors and of raising the degeneracy of the $(2L + 1)$ sublevels associated with a given value of L. If the ligand field results in an orbital singlet ground state, there should theoretically be no orbital contribution. However, spin-orbit coupling permits "mixing" of the ground state wave functions with those of the various excited states giving rise to a small orbital contribution. The extent of this mixing is dependent on the magnitude of the spin-orbit coupling constant λ and on the energy separation of the states involved. When the latter are of approximately equal magnitude ($\simeq KT$), this mixing can lead to a significant deviation from (3).

The basic formula for calculating magnetic susceptibilities has been derived by Van Vleck⁴²

$$\chi = N \frac{\sum_i \left[\left(\frac{E_i^{(1)2}}{KT} - 2E_i^{(2)} \right) e^{-E_i^O/KT} \right]}{\sum_i e^{-E_i^O/KT}} \quad (5)$$

where the E_i^O are zero-field energies and the $E_i^{(1)}$ and $E_i^{(2)}$ coefficients of the first and second order Zeeman effects respectively. (See Fig.3.3). Here

$$E_i^{(1)} = \langle \Phi_i | \mu | \Phi_i \rangle \quad (6)$$

$$E_i^{(2)} = \frac{\sum_j \langle \Phi_i | \mu | \Phi_j \rangle^2}{E_i - E_j} \quad (7)$$

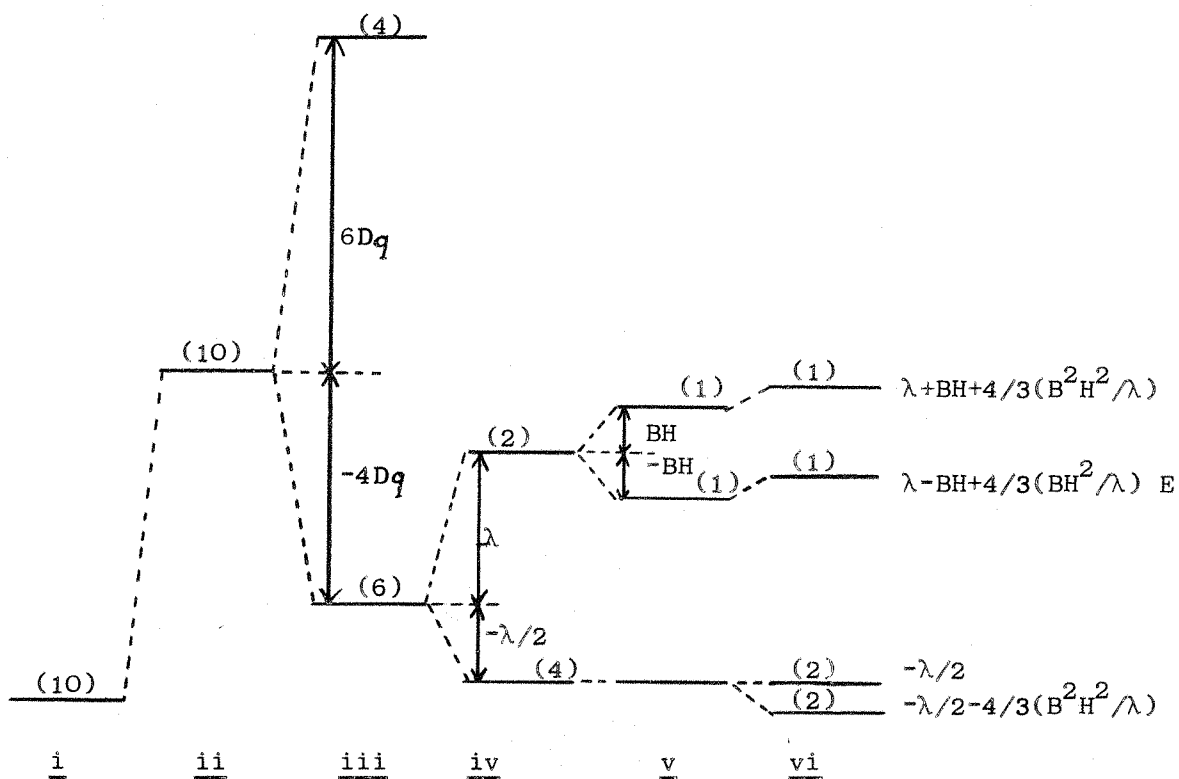
and μ is the Zeeman operator ($\beta(L + 2S)$). It has been found⁴³ that

to fit the temperature dependence of many measured susceptibilities it is necessary to use a modified operator

$$\mu = \beta(KL + 2S). \quad (8)$$

The parameter k provides a means for taking into account the fact that the orbital in which the unpaired electron is located is not localized entirely on the metal ion (i.e. The bond possesses some covalent character).

FIGURE 3.1



Changes in the energy levels of a d^1 ion (i) under the successive influence of a spherical potential (ii) a ligand field of O_h symmetry (iii) spin-orbit coupling (iv) and the first- (v) and second-order (vi) Zeeman effects. Not to scale. Numbers in parentheses are the total degeneracy of the level.

As with the absorption of light, the magnetic susceptibility of a compound may be anisotropic in the presence of a ligand field of non-cubic symmetry. Expressions completely analogous to (5), (6), and (7) can be written for the susceptibilities parallel to and perpendicular to the applied magnetic field, where the operators now take the form

$$\underline{\mu}_{\parallel} = (k\beta L_z + 2S_z) \quad (9a)$$

$$\underline{\mu}_{\perp} = (k\beta L_x + 2S_x) = \left[\frac{k\beta}{2} (L_+ + L_-) + (S_+ + S_-) \right] \quad (9b)$$

The effective magnetic moment is related to χ by

$$\mu^2 = \frac{3kT}{N\beta^2} \chi \quad (10)$$

where k is now Boltzmann's constant.

CHAPTER 4

PRELIMINARY X-RAY WORK

(i) Preparation and characterization of the crystals.

Crystals of hexaureatitanium(III) iodide were prepared according to the method of Hartmann et. al.⁴ The product was analyzed for Ti(III) and I⁻ in the manner outlined in the same reference, while C, N and H were determined by commercial micro-analysis (Microanalytical Section, Department of Chemistry, University of Reading). Oxygen was determined by difference from 100%.

For $[\text{Ti}(\text{CON}_2\text{H}_4)_6]\text{I}_3$ calc.--I⁻:48.25%, Ti(III):6.07%,
C:9.13%, N:21.31%, H:3.07%, O:12.17%
found--I⁻:48.31%, Ti(III):6.02%, C:9.11%,
N:21.24%, H:3.28%, O:12.1%.

The complex crystallizes as dark blue, well formed, hexagonal needles. Some of these are very nearly regular hexagons in cross section, while others have alternate faces prominently developed. When developed, the end faces formed an angle of $\sim 120^\circ$ with the needle axis. (See figure 4.1). Several crystals were employed for the photographic confirmation of space group and unit cell parameters (see below), but the crystal on which all intensity data were collected was of the type B shown in figure 4.1 but without well developed end faces. The overall dimensions of this crystal were 0.14 mm x 0.35 mm.

The crystal density was taken to be the pycnometrically determined value of 2.06 g/cm^3 reported in the literature.⁴

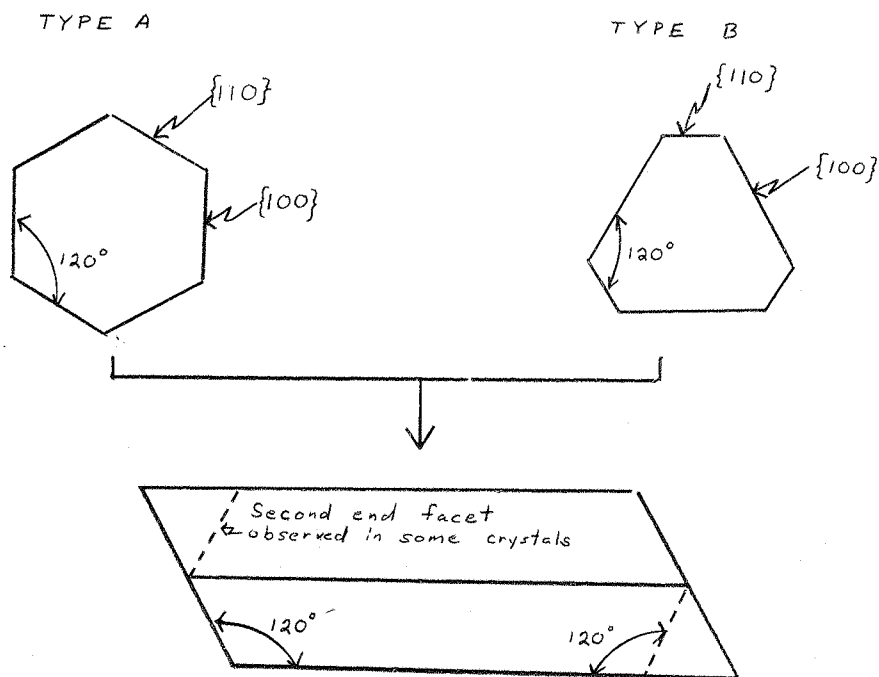


Figure 4.1. CRYSTAL MORPHOLOGIES

(ii) Determination of space group and unit cell parameters.

In order to confirm the reported²⁰ space group and unit cell parameters ($R\bar{3}c$, $a = 17.72\text{\AA}$, $c = 14.26\text{\AA}$) zero level precession photographs were recorded for the $h0l$ and hhl (diagonal) zones. Zirconium filtered molybdenum ($k\alpha$) radiation was used, since, although a large unit cell was indicated, the anticipated systematic absences would not have allowed the recording of a sufficient number of reflections with copper radiation.

In contrast to the anticipated three-fold symmetry, both sets of photographs exhibited six-fold symmetry. No consistent set of systematic absences could be discerned and it was not possible to index the reflections on the basis of any of the hexagonal groups.

It is interesting to note that in the original paper Hartmann *et al.*⁴ report that it was not possible to index a powder photograph of the complex, but that on the basis of equatorial Weissenberg photographs the crystal must have at least trigonal if not hexagonal symmetry. Reflections in the $h0l$ set could be indexed on the basis of the reported space group if it were assumed that the crystal was a twin, the two crystals sharing a common c axis with one being in the obverse and one in the reverse orientation.

Three additional crystals were examined to find one which did not show signs of twinning. The systematic absences of the $h0l$ zone photographs of the fourth crystal were consistent with the space groups $\bar{R}3c$ or $R3c$ (hkl absent for $-h+k+l \neq 3n$, $h0l$ absent for $l \neq 2n$). However, the hhl zone photographs contained a large number of extraneous reflections. The most prominent reflections in this zone could be indexed on the basis of the space groups $\bar{R}3c$ or $R3c$ with the unit cell parameters derived from the $h0l$ photographs and it was finally decided that the remainder were due to upper level reflections not completely cut off by the layer level screen. This last conclusion was supported by the following observations: 1) Considered by themselves, sets of the extraneous spots lead to the same cell dimensions as those determined from the $h0l$ photographs, 2) the extra sets of reflections occurred at regular intervals along the l axis, being situated at $1/3$ and $2/3$ the distance between rows of the most prominent reflections, and 3) the extra reflections were not as elongated parallel to l as the more prominent reflections (as if they had been "cut off") and choice of a new precession angle which permitted moving the layer level screen closer to the film, effectively

reducing the width of the screen gap, decreased the size and/or intensity or completely eliminated the extra reflections, while not noticeably affecting the more prominent ones.

Direct measurement of reciprocal lattice spacings on the zero level photographs lead to the following initial cell dimensions

$$a = 17.65\overset{\circ}{\text{\AA}}$$

$$c = 14.17\overset{\circ}{\text{\AA}}.$$

The crystal was now mounted on an eucentric goniometer head and transferred to a General Electric XRD-5 Manual Diffractometer. The crystal was centered using known methods⁴⁴ and the preliminary cell parameters used as an aid in locating the axial reflections. A refined set of cell parameters was determined on the basis of the 006, 0012, and 0018 (k_{a1} and k_{a2}) reflections for c and 030 and 060 for a. The approximate value of θ was determined by means of a 2θ scan and fixed time counts (100 seconds) at intervals of 0.01° in 2θ then used to determine the exact location of the maxima. The unit cell dimensions determined in this manner and the calculated density assuming six formula units in the unit cell are

$$a = 17.67\overset{\circ}{\text{\AA}}$$

$$c = 14.15\overset{\circ}{\text{\AA}}$$

$$\rho = 2.03 \text{ g/cm}^3.$$

(iii) Conditions of data collection.

Angle settings for the diffractometer were calculated on the basis of the above parameters using the GESET link of the X-RAY 63 system at the Imperial College Computing Center.

All data were collected using Zr-filtered Mo- k_{α} radiation with a scintillation tube detector and employing the moving crystal-moving counter technique. The x-ray source was a General Electric CA-8-S/Mo small focal spot tube and was operated at ca. 45 kv and 15 ma. Stability of the primary beam was checked by measuring the intensity of a standard reflection after each group of approximately ten reflections. Measurement of the 006 and 0012 reflections at $\chi = 90^{\circ}$ showed that they did not vary appreciably with ϕ through the range in which the data were collected. A complete set of data ^{was recorded} for

$$0 < 2\theta \leq 45^{\circ}$$

$$0 \leq \phi \leq 60^{\circ}$$

$$0 \leq \chi \leq 90^{\circ}$$

as well as approximately 200 symmetry related reflections in the sector $-60 < \phi < 0$ for the same limits on χ and 2θ .

CHAPTER 5

X-RAY STRUCTURE DETERMINATION AND REFINEMENT

(i) Preliminary treatment of data.

All calculations were carried out using the X-RAY 63 system of x-ray crystallographic programs and the facilities of the Atlas Computer Laboratory.

Data for 529 independent reflections were included in the refinement. Of these, 30 had net intensities equal to or less than the calculated standard deviation of the measurement (see Appendix B.) and were coded as "less thans".

The scattering factors used for all non-hydrogen atoms were those due to Cromer and Waber,⁴⁵ while those of Stewart, Davidson, and Simpson⁴⁶ were used for hydrogen. All intensities were corrected for Lorentz and polarization factors. The dispersion corrections for titanium and iodine for Mo-k_α radiation are small⁴⁷ and were not included.

The linear absorption coefficient, μ_L , is defined as

$$\mu_L = \rho \sum_n P_n (\mu_M)_n \quad (1)$$

where ρ is the crystal density, P_n the fractional weight of the element n in the compound, and μ_M the mass absorption coefficient of the element n for the wave length of radiation employed.

Although for Mo-k_α radiation, μ_L for hexaureatitanium(III) iodide calculated using the μ_M tabulated in the International Tables for X-Ray Crystallography⁴⁷ is only 40.77 cm⁻¹ it was felt that an absorption correction might be necessary due to the large difference

between the dimensions of the crystal parallel to and perpendicular to the needle axis. Absorption corrections were calculated for the individual F_{rel} using the ABSCOR link of X-RAY 63. ABSCOR is a modification of a program by De Muelenaer and Tompa⁴⁸ based on a technique originally suggested by Busing and Levy.⁴⁹ The transmission factors (defined by $F_{rel}(corr.) = F_{rel}/\text{transmission}$) varied only from 0.8049 to 0.8224.

- (ii) Determination of positions of non-hydrogen atoms and initial refinement.

Iodide and titanium together compose over 50% of the scattering matter in the unit cell and correct determination of their positions should determine a sufficient number of phases to allow a preliminary Fourier synthesis to be carried out, although both are constrained by symmetry to be situated on special positions and the titanium atom will contribute to only half of the reflections.

Within the space group $R\bar{3}c$ there are two separate sets of special positions of six-fold multiplicity, designated a (point symmetry $\bar{3}2$) and b (point symmetry $\bar{3}$), on which the titanium atoms may be located, and likewise, two sets of special eighteen-fold positions, designated d (point symmetry $\bar{1}$) and e (point symmetry 2), on which the iodide ions may be situated. Linek et. al.²⁰ have assigned the titanium to the a positions and iodide to the e positions.

Consideration of the coordinates of these positions (Table 5.1 below) will show that it should be possible to assign atomic positions for titanium and iodide unambiguously on the basis of a three-dimensional Patterson synthesis. It will be noted that whereas the coordinates of the special positions d are entirely fixed by symmetry, one coordinate of the set e is free. In addition,

TABLE 5.1
COORDINATES OF SPECIAL SIX-FOLD AND EIGHTEEN-FOLD
POSITIONS IN THE SPACE GROUP $R\bar{3}c$.^{* 47}

a: 0,0,1/4	d: 1/2,0,0	e: X,0,1/4
0,0,3/4	0,1/2,0	0,X,1/4
	1/2,1/2,0	$\bar{X},\bar{X},1/4$
b: 0,0,0	1/2,0,1/2	$\bar{X},0,3/4$
0,0,1/2	0,1/2,1/2	0, $\bar{X},3/4$

* Coordinates of additional equivalent positions may be obtained by adding (1/3,2/3,2/3) or (2/3,1/3,1/3) to any of the above coordinates.

determination of the possible I-I' vectors within the two sets will show that many fewer orientations are possible within the d set which will result in vectors of greater multiplicity and, therefore, give rise to peaks of greater height if this is actually the correct set. Accordingly, a three-dimensional Patterson synthesis was carried out within the limits $0 \leq x \leq 1$ (in units of 1/40), $0 \leq y \leq 1$ (in units of 1/40), and $0 \leq z \leq 1/3$ (in units of 1/60).

To a good approximation, the volume under a peak in the Patterson function is proportional to the peak height, and it is possible to estimate the height, H_{ij} , to be expected for a vector between two atoms i and j according to the formula

$$H_{ij} = m \frac{H_{ii}}{\sum_i z_i^2} z_i z_j \quad (2)$$

where H_{ii} is the height of the peak at the origin, the z_i the

atomic numbers of the various atoms, and m the vector multiplicity. In the present case the height of the origin peak (measured from the lowest trough) was 1964 so that $H_{ii} \sum z_i^2 = 1/32$. On this basis an I-I' vector of multiplicity 6 (the maximum within the set e) would have an anticipated height of 546, while one of multiplicity 18 (the maximum within the set d) would have an anticipated height of 1638. No peak of anywhere near the latter size was observed, while a set of peaks was observed which were of an appropriate magnitude and had the proper symmetry (assuming $x = 15/40$) to be attributed to I-I' vectors within the e set.

Having confirmed the location of the iodide ions on the special positions e, the location of a number of peaks with appropriate magnitudes and symmetry for Ti-I vectors in the planes $z=0$ and $z=1/6$ confirmed also the correctness of the assignment of titanium to the positions a.

The positions of titanium and iodide were now used as the basis of a Fourier synthesis calculated between the limits $0 \leq x \leq 1/3$ (in units of $1/45$), $0 \leq y \leq 2/3$ (in units of $1/45$), and $0 \leq z \leq 1/2$ (in units of $1/48$). Peaks corresponding to all non-hydrogen atoms in the urea molecule appeared in this synthesis. Peaks, including that from iodide, were contoured at arbitrary intervals and the atomic positions estimated. The resultant model was used as the basis of a least squares refinement. Two cycles of full-matrix least squares refinement varying the overall scale factor, all positional parameters not fixed by symmetry, and individual atom isotropic temperature factors with unit weight assigned to all observed reflections produced

a conventional weighted residual of 0.120.*

As previously noted (See Chapter 2), the finite size of an atom gives rise to an atomic scattering factor which is a decreasing function of $\sin\theta/\lambda$. The scattering factors normally tabulated are calculated for atoms assumed to be at rest. In a molecule the atoms may be assumed to be vibrating about some equilibrium position. This will have the effect of "smearing out" the electron density, causing the scattering factor to fall off even more rapidly and it is necessary to introduce an additional term into the scattering factor expression which takes this effect into account. It is obvious that this factor will be a function of the vibrational displacements. In the first approximation these are assumed to be isotropic and the temperature factor by which the scattering factor must be multiplied is given by

$$T.F. = e^{-B \sin^2 \theta / \lambda^2} = e^{-B/4d^2} \quad (3)$$

where d is the interplanar spacing and B is related to the root mean square amplitude of vibration $\overline{u^2}$, by

$$B = 8\pi^2 \overline{u^2} \quad (4)$$

In the second approximation, the constraint that the vibrational amplitudes to be isotropic is dropped, resulting in an ellipsoid of vibration rather than a sphere. In three-dimensional space six parameters are necessary to determine an ellipsoid (e.g. The lengths

* A commonly used index of the degree of agreement between the postulated and "actual" structures is the weighted residual, or R factor, defined as:

$$R = \left[\frac{\sum_i w_i (F_{oi} - |F_{ci}|)^2}{\sum_i w_i |F_{oi}|^2} \right]^{1/2}$$

of the three principal axes of the ellipse and the angles between these axes and some reference coordinate system) and the general anisotropic temperature factor will contain six terms. These may also be considered as corresponding to the six terms in the expression for $1/d$, and one commonly used form of the general anisotropic temperature factor is

$$\begin{aligned} \text{T.F.} = & \left[-1/4(B_{11}h^2a^{*2} + B_{22}k^2b^{*2} + B_{33}l^2c^{*2} + 2B_{12}hka^*b^*\cos\gamma^* + \right. \\ & \left. 2B_{13}hla^*c^*\cos\beta^* + 2B_{23}klb^*c^*\cos\alpha^*) \right] \end{aligned} \quad (5)$$

where the starred quantities are the usual reciprocal cell parameters and the B_{ij} 's the anisotropic thermal parameters.

For an atom on a special position, the vibrational ellipsoid must conform to the point symmetry of the site. In such a case some of the B_{ij} in (5) may be constrained to take on specific values, or two or more of them may be related in some specific way. If one were to try to vary these parameters independently, the coefficient matrix of the resulting normal equations would become singular. Since in the present case both titanium and iodide are located on special positions, it was necessary to write a "patch" for the full-matrix least squares refinement program before refinement in the anisotropic mode could be undertaken. Details of the specific relations between the B_{ij} and an outline of the "patch" program may be found in Appendix C.

Two cycles of full-matrix least squares refinement varying the overall scale factor and all independent positional and anisotropic thermal parameters with unit weight for all reflections reduced the weighted R factor to 0.090.

- (iii) Determination of positions of hydrogen atoms and final refinement.

At this stage of the refinement a difference Fourier synthesis was carried out in an attempt to locate the four independent hydrogen atoms of the urea molecule. Six regions with an electron density excess of $0.5 \text{ electron}/\text{\AA}^3$ or more were observed. Two of these were located within $\sim 1.25 \text{ \AA}$ of the position of the titanium atom and were not considered further. The remaining peaks were contoured at arbitrary intervals and the distance from their centers to the nearest nitrogen atom calculated. One of the regions contained two distinct maxima and the N-peak distance was calculated for both. Two of the peaks, including one of the maxima of the double peak were found to be $\sim 1.0 \text{ \AA}$ from one of the nitrogen atoms and were tentatively assigned to two hydrogen atoms. The remaining two peaks were $2.5 - 3.0 \text{ \AA}$ from the nearest nitrogen and were assumed not to be due to hydrogen. No immediate explanation of their origin was obvious.

On the basis of the positions which had been established, a model of the urea molecule was constructed. In agreement with studies^{50,51} of free urea, the molecule, including the tentatively positioned hydrogen atoms, was found to be planar. The probable positions of the remaining hydrogen atoms were estimated assuming coplanarity with those portions of the molecule already determined, an N-H bond of 1.0 \AA , and bond angles about the nitrogen of 120° . The difference Fourier map was searched in the predicted positions and two regions showing an electron density excess of $0.4 \text{ electrons}/\text{\AA}^3$ located. These were contoured and their centers taken as the positions of the remaining hydrogen atoms.

The hydrogen atom positions were added to the model and the hydrogens assigned isotropic temperature factors equal to those of the nitrogens to which they were bound (taken as the value at the end of isotropic refinement).

A weighting scheme based on the calculated standard deviations in the F_{rel} derived from counting statistics (see Appendix B), was now introduced. Two cycles of full-matrix least squares refinement varying the overall scale factor and all independent positional and thermal parameters for non-hydrogen atoms reduced the R factor to 0.082. At this time nine reflections showing signs of being affected by secondary extinction (i.e. $\sin\theta/\lambda < \sim 0.17$, large $|F_c|$, and $|F_c| \gg |F_o|$) were removed from the data set. A further two cycles of full-matrix least squares refinement as above reduced the weighted R factor for the observed reflections to 0.064 (0.097 including "less thans") at which point convergence was assumed. The R factor did not change during the final cycle and no parameter changed by more than 0.181 of its estimated standard deviation, while the average shift/error for the 44 parameters refined on was 0.063. A difference Fourier synthesis showed no region of electron density excess or deficiency exceeding 0.3 electrons/A^{o3} and the largest of these were associated almost exclusively with the position of titanium and iodide. In the regions of the assumed positions of the hydrogen atoms the maximum deviations were ± 0.15 electron/A^{o3}.

(iv) Summary of structural information.

The final structural information is summarized in figures 5.1 and 5.2 and tables 5.2-5.6. A listing of the final observed and calculated structure factors will be found in Appendix A.

In considering the coordination geometry, the oxygen atoms are found to be situated at the vertices of a slightly distorted octahedron. The form of this distortion is most evident when the molecule is viewed in projection along the three-fold axis. In this view the three oxygen atoms above the plane of the titanium are seen to be rotated about this axis with respect to the set of oxygen atoms below the titanium. Regular octahedral geometry requires that the angle between successive Ti-O bonds projected onto the xy-plane be 60° , while in the complex this angle is observed to be 54.45° . In contrast, the form of trigonal distortion usually assumed, that of compression or extension along the three-fold axis, is virtually absent, the angle between a Ti-O bond and this axis being $55.07 \pm 0.13^\circ$ compared to 54.75° required by regular octahedral geometry.

A Ti-O-C bond angle of $\sim 120^\circ$ was previously reported.²⁰ This differs greatly from the value of $138.36 \pm 0.48^\circ$ found in the present study. The previous determination was made in projection along c. The projection of this angle onto the xy-plane is 115.33° and the overlap, when viewed in this projection, between carbon and nitrogen atoms in ligand molecules above and below the plane of the titanium (see figure 5.1) would make accurate determination of this angle from a two dimensional analysis difficult.

Reference to Table 5.6 will show that the geometry of the urea molecule in the complex is essentially the same as that of the free urea molecule. Since no attempt was made to refine the positions of the hydrogen atoms, only rough comparisons can be made for bond lengths and angles involving these atoms. There does,

however, appear to be a slight but significant difference in the two C-N bonds in the ligand molecule. This may be the result of intramolecular hydrogen bonding involving the urea molecules coordinated to a single titanium. One of the hydrogens bound to the nitrogen involved in the shorter of the two bonds is hydrogen bonded to the oxygen atoms in two separate urea molecules ($\text{H}\cdots\text{O}$ distances 2.77 and 2.27 Å; see figure 5.1). Hydrogen bonding to the iodide ions also appears to take place. The bonds between hydrogen atoms of types (11) and (21) (see figure 5.1), and the iodide ions with the same z coordinate as the titanium are relatively weak ($\text{H}\cdots\text{I}$ distances 3.50 and 3.58 Å), but those between hydrogen atoms of the type (22) and the iodide ions with z coordinates differing from that of the titanium by $\pm 1/6$ are quite strong ($\text{H}\cdots\text{I}$ distance 2.79 Å). The bound urea molecule is essentially planar, three of the hydrogen atoms being less than 0.2 Å out of the plane formed by the four heavier atoms. (The maximum deviation of one of the heavy atoms from the plane is 0.01 Å). The titanium atom lies slightly out of the plane of the urea molecule.

Although associated with each titanium are three iodide ions with the same z coordinate, the closest $\text{Ti}\cdots\text{I}$ approach is actually made by those iodide ions whose z coordinates differ from that of the titanium by $\pm 1/6$ (6.077 and 6.069 Å vs. 6.515 Å). Thus any attempt to consider the effect of second nearest neighbors on the ligand field potential would require consideration of the entire set of nine iodide ions. Because the x coordinate of the iodide special positions is very nearly 1/3, spiral chains which are very nearly linear are formed parallel to the z axis by iodide ions separated by 1/3 in z.

FIGURE 5.2

The $[\text{Ti}(\text{CO}(\text{NH}_2)_2)_6]^{3+}$ ion projected onto (010),

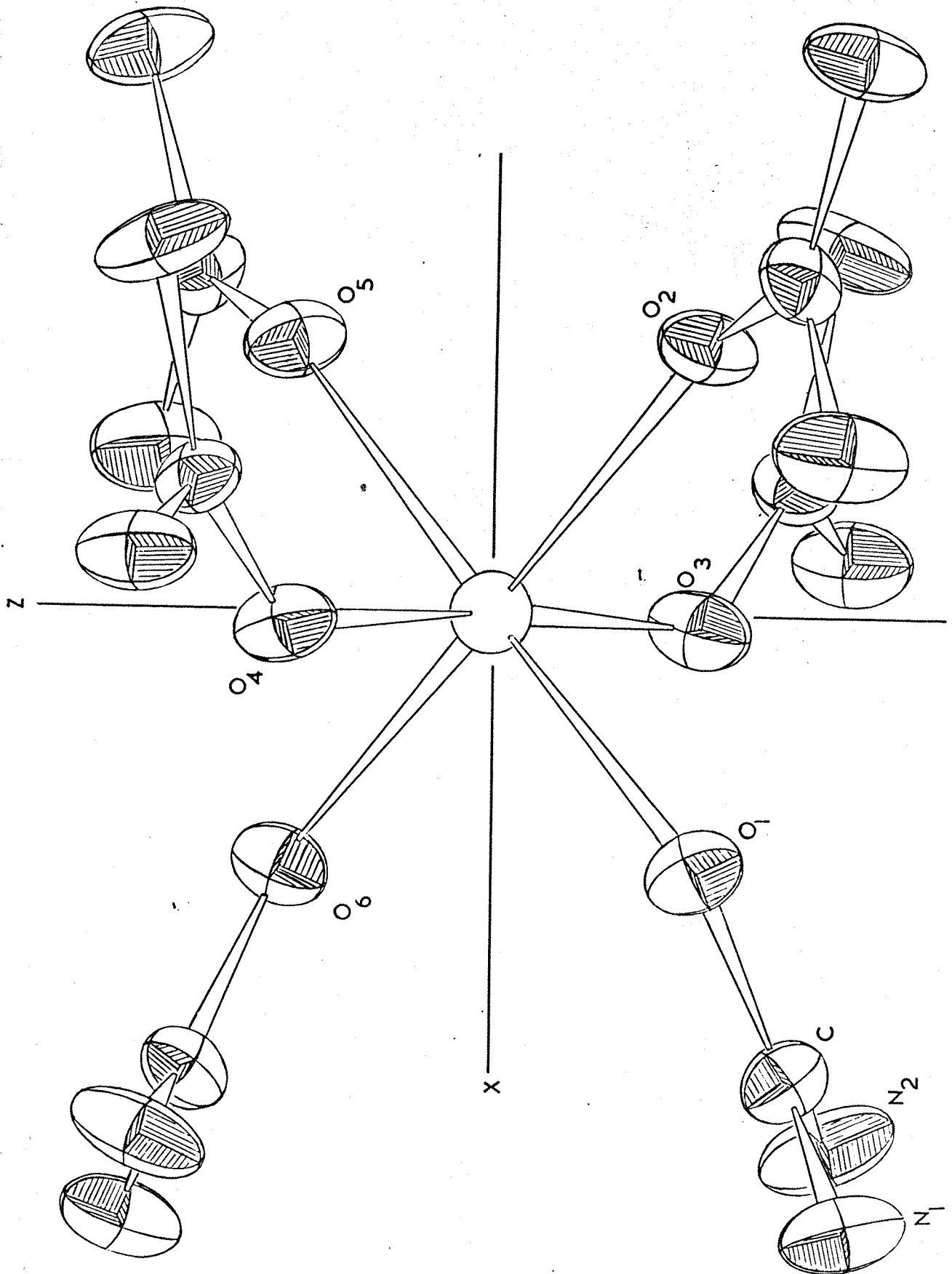


TABLE 5.2

FINAL POSITIONAL PARAMETERS (IN FRACTIONAL COORDINATES)^a

FOR $[\text{Ti}(\text{CO}(\text{NH}_2)_2)_6]\text{I}_3$

ATOM ^b	X	Y	Z
Ti	0.00000	0.00000	0.25000
I ⁻	0.37023(4)	0.00000	0.25000
O	0.10778(31)	0.05841(28)	0.16850(37)
C	0.16334(47)	0.04070(45)	0.13311(49)
N ₁	0.23977(41)	0.10298(46)	0.11011(67)
N ₂	0.14422(45)	-0.04170(42)	0.11655(70)
H ₁₁	0.2867 ^c	0.0889	0.0875
H ₁₂	0.2400	0.1578	0.1188
H ₂₁	0.1828	-0.0565	0.1052
H ₂₂	0.0890	-0.0811	0.1481

^a Estimated standard deviations in last significant digits.

^b See figure 5.1 for numbering of atoms.

^c As hydrogen atom positional parameters were not refined, no estimated standard deviations are available.

TABLE 5.3
FINAL ANISOTROPIC THERMAL PARAMETERS (\AA^2) FOR
 $[\text{Ti}(\text{CO}(\text{NH}_2)_2)_6]\text{I}_3$

ATOM ^b	B ₁₁	B ₂₂	B ₃₃	B ₁₂	B ₁₃	B ₂₃
Ti	4.63(18)	4.63(18)	3.82(17)	2.32(9)	0.00	0.00
I ⁻	6.26(8)	3.66(6)	5.64(7)	1.83(3)	-0.37(1)	-0.75(1)
O	3.48(22)	2.90(24)	5.04(27)	1.53(18)	0.68(19)	-0.16(19)
C ₁	3.34(36)	3.35(35)	3.73(36)	1.83(31)	0.93(28)	-0.05(28)
N ₁	3.55(33)	3.61(31)	8.16(50)	1.88(27)	1.53(30)	0.52(33)
N ₂	3.99(31)	3.93(35)	10.43(60)	1.36(30)	-3.66(37)	-1.47(35)
H ₁₁	4.00 ^c	4.00	4.00	2.00	0.00	0.00
H ₁₂	4.00	4.00	4.00	2.00	0.00	0.00
H ₂₁	4.50	4.50	4.50	2.25	0.00	0.00
H ₂₂	4.50	4.50	4.50	2.25	0.00	0.00

^a Estimated standard deviations in last significant digits.

^b See figure 5.1 for numbering of atoms.

^c As hydrogen atom thermal parameters were not refined, no estimated standard deviations are available.

TABLE 5.4

ROOT MEAN SQUARE AMPLITUDES OF VIBRATION (IN Å)^a
ALONG THE PRINCIPAL AXES OF THE THERMAL ELLIPSOID

ATOM ^b	MAJOR AXIS	MED. AXIS	MINOR AXIS
Ti	0.2422(63)	0.2422(63)	0.2199(44)
I ⁻	0.3004(27)	0.2731(13)	0.2079(11)
O	0.2628(68)	0.2020(74)	0.1892(71)
C	0.2407(102)	0.2067(108)	0.1693(100)
N ₁	0.3306(100)	0.2122(91)	0.1953(99)
N ₂	0.3923(105)	0.2463(95)	0.1680(111)
H ₁₁	0.225 ^c	0.225	0.225
H ₁₂	0.225	0.225	0.225
H ₂₁	0.239	0.239	0.239
H ₂₂	0.239	0.239	0.239

^a Estimated standard deviations in last significant digits.

^b See figure 5.1 for numbering of atoms.

^c As hydrogen atom thermal atom parameters were not refined, no estimated standard deviations are available.

TABLE 5.5

MOLECULAR GEOMETRY

A. BOND LENGTHS (IN Å)^a

BOND	LENGTH	BOND	LENGTH
Ti-O	2.0141(50)	N ₁ -H ₁₁	1.0277(68)
C-O	1.2727(86)	N ₁ -H ₁₂	0.9760(72)
C-N ₁	1.2858(98)	N ₂ -H ₂₁	0.8921(69)
C-N ₂	1.3307(95)	N ₂ -H ₂₂	0.9558(76)

B. BOND ANGLES^a

ATOMS ^{b,c}	ANGLE	ATOMS	ANGLE
Ti-O-C	138.36(48)	O-C-N ₁	119.94(70)
O ₁ -Ti-O ₂	90.47(8)	O-C-N ₂	120.63(70)
O ₁ -Ti-O ₄	86.39(29)	N ₁ -C-N ₂	119.38(75)
O ₁ -Ti-O ₆	92.84(26)	C-N ₁ -H ₁₁	120.15(73)
Ti ^f -Ti-O	55.07(13)	C-N ₁ -H ₁₂	107.35(71)
(angle between a Ti-O bond and the three-fold axis)		H ₁₁ -N ₁ -H ₁₂	132.50(98)
O ₁ -Ti-O ₄	54.45	C-N ₂ -H ₂₁	121.71(81)
(projected onto the xy-plane)		C-N ₂ -H ₂₂	110.50(74)
		H ₂₁ -N ₂ -H ₂₂	120.85(99)

^a Estimated standard deviations in the last significant digits.

^b See figure 5.1 for numbering of atoms.

^c The second named atom is at the vertex of the angle.

TABLE 5.6
LIGAND GEOMETRY

A. COMPARISON OF GEOMETRY OF BOUND AND FREE UREA

(i) INTERATOMIC DISTANCES^{a, b}

ATOMS	THIS WORK	CARON AND DONOHUE ⁵²	WORSHAM ET. AL. ⁵¹
O-C	1.273(9)	1.268(7)	1.243(6)
C-N	1.286(10)	1.326(6)	1.351(7)
	1.331(9)		
N-H ₁	1.028(7)		0.988(20)
	0.892(7)		
N-H ₂	0.956(8)		0.995(7)
	0.976(7)		
N-H(ave)	0.960		0.992

(ii) ANGLES^{a, b, c}

O-C-N	119.9(7)	121.0(3)	121.5(3)
	120.6(7)		
N-C-N	119.4(8)	117.9(6)	117.0(3)
H ₁ -N-C	120.2(7)		119.8(8)
	121.7(8)		
H ₂ -N-C	107.4(7)		118.1(9)
	110.5(7)		
H-N-H	132.5(10)		122.1(9)
	120.9(10)		

^a Estimated standard deviations in last significant digits.

^b Subscript numbering on H corresponds to second subscript in previous tables and figures.

^c Second named atom is at the vertex.

TABLE 5.6

(CONTINUED)

B. LEAST SQUARES PLANE PARAMETERS

Equation^a of best least squares plane through urea molecule (1);

$$0.3276X - 0.2396Y + 0.9140Z = 2.7019$$

Distances of atoms^b from plane:

Ti	0.531	^O A
O	-0.002	
C	0.012	
N ₁	-0.004	
N ₂	-0.004	
H ₁₁	0.097	
H ₁₂	-0.225	
H ₂₁	0.201	
H ₂₂	0.191	

^a In the orthogonal coordinate system used, Y and Z are coincident with the crystallographic Y and Z, and X is orthogonal to the YZ-plane forming a right-handed coordinate system.

^b See figure 5.1 for numbering of the atoms.

CHAPTER 6

INTERPRETATION OF SPECTRAL AND MAGNETIC PROPERTIES

- (i) Ligand field calculations based on the x-ray structure determination.

Previous studies of the spectral and magnetic properties of hexacoordinate complexes of titanium(III) (and of the other d^n -ions) have generally assumed an octahedral ligand field with the presence of lower symmetry components in the ligand field taken into account by the addition of a small perturbing potential to the primary cubic-field potential.

If one of the three-fold axes of the octahedron is taken to be the axis of quantization, the potential due to an octahedron of charges can be shown to be⁵³

$$V_{O_h} = Y_4^0 + \left(\frac{10}{7}\right)^{\frac{1}{2}}(Y_4^3 - Y_4^{-3}) \quad (1)$$

The splitting of the free-ion D- and F-terms under such a potential is conveniently expressed in terms of the parameter Dq . If a distortion of the octahedron by compression or extension along this three-fold axis is assumed, the Y_4^0 term of the potential is modified and an additional term dependent on the second order spherical harmonic Y_2^0 is introduced

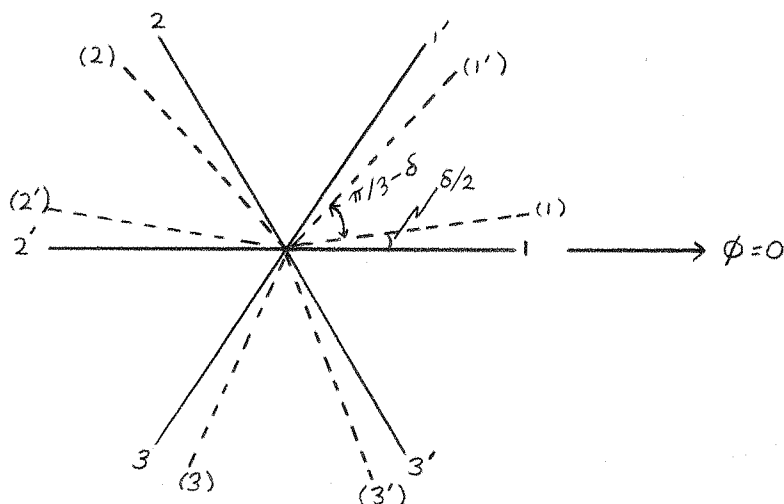
$$V_{\text{trig}} = V_{O_h} + aY_2^0 + bY_4^0 \quad (2)$$

The single parameter Dq is no longer sufficient to describe the

splitting of the free-ion terms and a second parameter (e.g. See Figgis⁵⁴) is introduced.* A second form of trigonal distortion, "twisting" of the opposite faces of the octahedron through some angle δ about the three-fold axis is possible (See figure 6.1).

FIGURE 6.1

THE "TWIST" DISTORTION



The full lines indicate the angular positions of the ligands in a regular octahedron, the broken lines those in an octahedron whose opposite faces have been twisted with respect to one another through a total angle δ about the three-fold axis. The z-axis is out of the plane of the paper. The unprimed numbers indicate ligands above the plane of the paper; the primed numbers ligands below the plane.

*

Gerloch and Slade⁵⁷ have recently showed that in the case of "tetrahedral" nickel(II) complexes (d^8 -ion, 3T_1 cubic-field ground term) the trigonal potential is dominated by the Y_4^0 term. They have found that the splitting of the ground term is essentially independent of the contribution from the Y_2^0 term so that the parameter Dq is sufficient to specify the 2 ligand field. Preliminary calculations for "octahedral" d^1 - and d^2 -ions indicate that the result may be more general.

It is this latter form of distortion which is observed to be most important in the case of the hexaurea titanium(III) ion in the iodide salt. The potential calculated for this configuration is identical in form to (1) which coincidence seems to have led Figgis⁵⁴ to assume that it does not further split the cubic-field terms. That this is not so can be seen by writing (1) in a form which takes into account the explicit form of the angular dependence of the spherical harmonics.

$$V_{\text{twist}} = K_0(35\cos^4\theta - 30\cos^2\theta + 3) + K_3(\sin^3\theta \cos\theta \cos 3\phi) \quad (3)$$

For the regular octahedral case the polar coordinate ϕ will take on the values $0, 2\pi/3$, and $4\pi/3$ for one set of ligands and $\pi/3, \pi$, and $5\pi/3$ for the other, while for the twist distortion these angles will assume the values $\delta/2, 2\pi/3 + \delta/2, 4\pi/3 + \delta/2$ and $\pi/3 - \delta/2, \pi - \delta/2, 5\pi/3 - \delta/2$ respectively (See figure 6.1). In the former case $\cos 3\phi$ will always equal ± 1 , while in the latter this factor will, in general, be different from 1. The secular determinant for the effect of V_{twist} on the d-wave functions is

$$\begin{array}{c|ccccc|c} 2 & -2/3Dq-E & 0 & 0 & \beta & 0 & \\ 1 & 0 & 8/3Dq-E & 0 & 0 & -\beta & \\ 0 & 0 & 0 & 4Dq-E & 0 & 0 & \\ -1 & \beta & 0 & 0 & 8/3Dq-E & 0 & \\ -2 & 0 & -\beta & 0 & 0 & -2/3Dq-E & \\ \hline & & & & & & =0 \quad (4) \end{array}$$

where the labels along the left-hand side refer to the m_l values of the relevant d-orbitals and where $\beta = 2/3(50)^{1/2}\cos 3\phi$. The matrix (4) may be reduced to

$$O|4Dq-E| = 0 \quad (4a)$$

and

$$\begin{vmatrix} 2 & -2/3Dq-E \beta \\ -1 & \beta \end{vmatrix} = \begin{vmatrix} 1 & 8/3Dq-E -\beta \\ 2 & -\beta \end{vmatrix} = 0 \quad (4b)$$

which may be solved to give the energies

$$\begin{aligned} E_1 &= (1 + \sqrt{\frac{25}{9} + \frac{200}{9} \cos 3\phi})Dq \quad (|2\rangle, |-1\rangle \text{ and } (|1\rangle, |-2\rangle) \\ E_2 &= (1 - \sqrt{\frac{25}{9} + \frac{200}{9} \cos 3\phi})Dq \quad (|2\rangle, |-1\rangle \text{ and } (|1\rangle, |-2\rangle) \quad (5) \\ E_2 &= -4Dq \quad |0\rangle \end{aligned}$$

As can be seen, for ϕ not an integral multiple of $\pi/3$, this potential gives rise to, in order of increasing energy, an orbital singlet and two orbital doublets. Most importantly, it will be noted that all of the splittings are expressible in terms of the single parameter Dq . It thus becomes feasible to use as basis functions for further calculations the set of exact trigonal-field wave functions rather than the perturbed cubic-field set. The general form of these trigonal-field functions will be

$$\begin{aligned} \psi_1(a_1) &= |0\rangle \\ \psi_2(e^1) &= c_1|1\rangle + c_2|-2\rangle \\ \psi_3(e^2) &= c_2|-1\rangle - c_2|2\rangle \\ \psi_4(e^{*1}) &= c_2|1\rangle - c_2|-2\rangle \\ \psi_5(e^{*2}) &= c_2|-1\rangle + c_1|2\rangle \end{aligned} \quad (6)$$

where the particular coefficients c_1 and c_2 may be found by substituting a specific value for ϕ into equations (5), substituting the resulting energies back into the secular equations, and applying the usual

normalization condition. For the regular octahedron $c_1 = (\frac{1}{3})^{\frac{1}{2}}$ and $c_2 = (\frac{2}{3})^{\frac{1}{2}}$.

From the x-ray structure determination δ is about 6° for the hexaureatitanium(III) ion in the iodide salt, while from spectral measurements Dq is about 1700 cm^{-1} . Thus the splitting between the ground state (a_1) and the first excited state (e) should amount to about 93 cm^{-1} .

(ii) Interpretation of spectral results.

As part of a study of the spectral and magnetic properties of complexes containing M^{3+} ions in trigonal environments, the polarized single crystal spectrum of hexaureatitanium(III) iodide has recently been reported.²² The spectrum consists of a single band centered at about 17000 cm^{-1} with two maxima split by about 2500 cm^{-1} . Although the low energy component is rather strongly π polarized, both components have a significant intensity in both π and σ polarizations. The only change observed on cooling the crystal to 4.2°K was a blue-shift of the low energy component, reducing the splitting to 1850 cm^{-1} . The titanium ion in hexaureatitanium(III) iodide had previously been reported to be located on a position of D_3 symmetry. In such an environment the ${}^2T_{2g}$ term of the ion in a cubic-field is further split to give a 2A_1 and a 2E term. The possible transitions now become $({}^2A_1, {}^2E) \rightarrow {}^2E$. Since this symmetry does not require a center of inversion, transitions within the d-orbital manifold would not formally be Laporte forbidden. The direct product representations of the relevant intensity integrals along with the resultant selection rules are presented below

$$\begin{array}{llll}
 \sigma : & A_1(xy)E & A_1 \times E \times E = A_1 + A_2 + E & \text{allowed} \\
 \pi : & A_1(z)E & A_1 \times A_2 \times E = E & \text{forbidden} \\
 \sigma : & E(xy)E & E \times E \times E = 3E + A_1 + A_2 & \text{allowed} \\
 \pi : & E(z)E & E \times A_2 \times E = A_1 + A_2 + E & \text{allowed}
 \end{array}$$

Since in the case of an A_1 ground state the transition should be forbidden in the π polarization while, in fact, this is observed to be the most intense transition, it was concluded that the 2E was the ground term. This is, however, at variance both with previous assignments based on magnetic susceptibility measurements and with the results of the ligand field calculations based on the structure determination of this work.

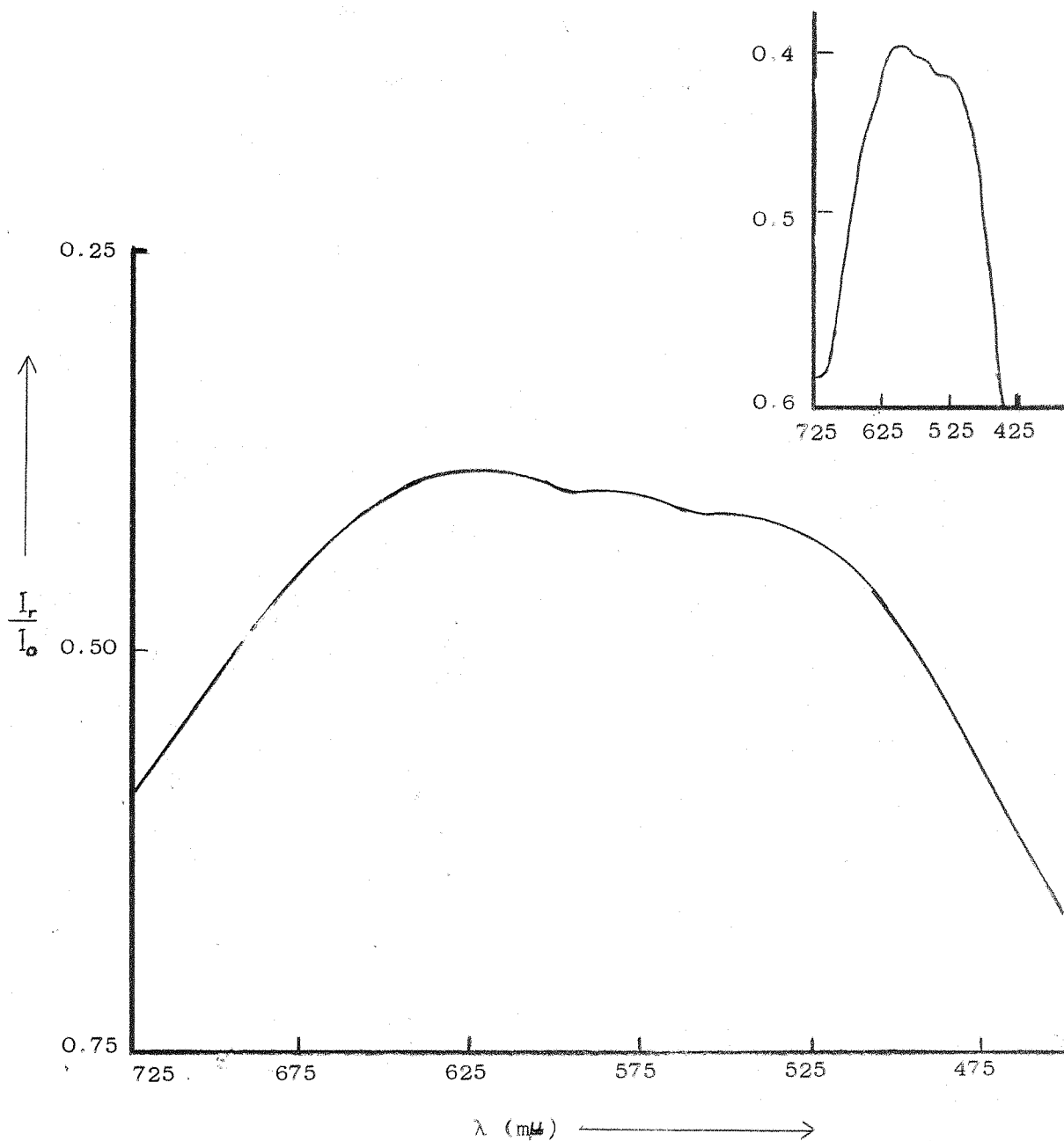
One possible explanation of this contradiction would appear to lie in the assumption that the transitions are purely electronic in nature. Liehr and Ballhausen⁵⁵ have showed that the oscillator strength of this transition is consistent with a vibronic intensity giving mechanism. In addition, it is widely accepted that the origin of the splitting of the absorption is the action of a dynamic Jahn-Teller effect on the excited state. The dynamic Jahn-Teller effect is in itself a manifestation of the interaction of the vibrational and electronic portions of the wave functions involved. The first excited states of the normal modes of vibration of the hexaureatitanium(III) ion will have the symmetries $3A_1$, $5E$, $2A_2$ and according to the rules governing vibronically allowed transitions, all transitions should be allowed in all polarizations. Alternatively, it may be necessary to have recourse to the complete double group D_3^* to establish the selection rules, since for the present case the ligand field splitting Δ and spin orbit coupling constant λ are of

similar magnitudes. Following the nomenclature of Ballhausen,⁵³ the 2A_1 term transforms as the two-fold degenerate Γ_6 of the double group, while the 2E term transforms like $\Gamma_4 + \Gamma_5 + \Gamma_6$, Γ_4 and Γ_5 remaining degenerate in the absence of a magnetic field. Formation of the direct products in the normal manner reveals that while transitions from the ground term to $(\Gamma_4 + \Gamma_5)$ are σ - polarized only, transitions to the Γ_6 component are allowed in both polarizations. While certainly not establishing the 2A_1 as the ground term, the above considerations serve to show that such an assignment is not inconsistent with the polarization results.

The diffuse reflectance spectrum of hexaureatitanium(III) iodide has been measured on the Bausch and Lomb Spectronic 600 and Unicam SP 700 spectrophotometers equipped with the appropriate reflectance attachments. In contrast to the solution and single crystal spectra, the characteristic d-d band appears to have three maxima, one at $17,000\text{ cm}^{-1}$ in addition to the two normally reported at $16,000$ and $18,000\text{ cm}^{-1}$ (See figure 6.2). The reflectance spectrum has previously been reported⁴ to be identical to the solution spectrum; however, it should be noted that this spectrum was recorded by a point-by-point rather than a continuous scan technique. It is not immediately obvious why the reflectance spectrum should differ from the other two, especially the single crystal spectrum. It is perhaps worth noting that a weighted average of the spectra obtained in the π and σ polarizations from the single crystal ($\bar{\epsilon} = 1/3(\epsilon_{||} + 2\epsilon_{\perp})$) reproduces both the positions and relative intensities of the three maxima.

FIGURE 6.2

REFLECTANCE SPECTRUM OF $[\text{Ti}(\text{CO}(\text{NH}_2)_2)_6]\text{I}_3$



The spectra were measured on a Bausch and Lomb Spectronic 600 equipped with the standard reflectance attachment. MgCO_3 was used as the standard. The inset spectrum is of the same sample run at a higher scan speed, emphasising the three maxima.

(iii) Interpretation of magnetic results.

The perturbation of a free-ion spectroscopic term by the combined influences of a ligand field, spin-orbit coupling, and an external magnetic field may be represented by the effective Hamiltonian

$$H = V_{LF} + \lambda L.S + \beta H(kL + 2S) \quad (7)$$

in which V_{LF} is the total ligand field potential, λ the effective spin-orbit coupling constant for the metal ion, and the parameter k in the Zeeman operator is Stevens' orbital reduction factor. The ligand field has already been considered. For the calculation of corrections to the energy levels and wave functions under the operation of spin-orbit coupling, the trigonal field wave functions were used as a basis set and the spin-orbit operator cast in the form

$$\lambda L.S = \lambda(L_z S_z + 1/2(L_+ S_- + L_- S_+)) \quad (8)$$

The complete secular determinant under this operator is given in Appendix D. The zero-order corrected energies were determined from a consideration of the elements coupling the functions of the 2A_1 ground term with those of the first 2E excited term (upper left-hand block of the secular determinant) and are found to be

$$\begin{aligned} E_1 &= -(3/2)^{1/2} \lambda c_1 \cot \theta \\ E_2 &= (2c_2^2 - c_1^2) \lambda / 2 + (3/2)^{1/2} \lambda c_1 \cot \theta + \Delta \\ E_3 &= (c_1^2 - 2c_2^2) \lambda / 2 + \Delta \end{aligned} \quad (9)$$

where Δ is the total splitting between 2A_1 and the first 2E and where

$$\tan\theta = 2\lambda c_1 (3/2)^{1/2} / [(c_1^2 - 2c_2^2)\lambda/2 - \Delta] \quad (10)$$

The corrections to the wave functions were determined using the full matrix, consideration of the non-zero off-diagonal terms outside the block considered above being necessary to allow for the mixing between the lower levels and the upper excited 2E term. Recent theoretical studies⁵⁶ have shown such effects to be significant for the magnetic properties of complexes, particularly for magnetic anisotropies.

For the evaluation of the magnetic properties of anisotropic systems it is necessary to use the Zeeman operators in the forms shown in equations (9a) and (9b) of Chapter 3. The principal and average susceptibilities may be calculated from Van Vleck's equation (equation (5) of Chapter 3) and the relation

$$\bar{\chi} = 1/3(\chi_{||} + 2\chi_{\perp}) \quad (11)$$

The principal and average moments follow from the relationship

$$\mu_{\text{eff}}^2 = \left(\frac{3kT}{N\beta^2} \right) \chi \quad (12)$$

A summary of the matrix elements of the first-order corrected wave functions under the operators $\mu_{||}$ and μ_{\perp} along with the expressions for the principal susceptibilities $\mu_{||}$ and μ_{\perp} will be found in Appendix D. Using the trigonal field wave functions calculated for an angular distortion of 6° and a value of 1700 cm^{-1} for Dq (values appropriate for hexaureatitanium(III) iodide), the principal and average magnetic moments were calculated for all possible combinations of $\lambda = \lambda_0, 0.5\lambda_0$ and $k = 1.0, 0.8, \dots, 0.4$ where λ_0 is the free ion spin orbit coupling constant for titanium(III) of 155 cm^{-1} . In

addition, the effect of an additional trigonal potential such as might arise from consideration of the potential due to the iodide ions was considered by allowing Δ , the splitting between the 2A_1 and first 2E terms under the ligand field potential, to take on the values Δ_0 , $1.5\Delta_0$, and $2.0\Delta_0$ where Δ_0 is the calculated splitting due to the twist potential. It should be noted that such a potential will "scramble" the two sets of e states, and, although the effect of such "scrambling" may be significant for the magnetic properties, the present treatment makes no allowance for such effects.

Some representative results are plotted in figures 6.3 - 6.5 where the calculated values of the average magnetic moment as a function of temperature are compared with the experimental values for hexaureatitanium(III) iodide over the range 100-300°K (Experimental points include values reported by Machin, Murray, and Walton²⁵ as well as measurements arising from the present study). The zero-order corrected energies and magnetic anisotropies for the set of parameters giving the best fit are also tabulated in Table 6.2. Several features of the results are worth noting. Regardless of the value of Δ , the best fit of calculated to experimental values is found for $\lambda = \sim 100 \text{ cm}^{-1}$ and $k = 0.4$ to 0.5 . Secondly, an essentially exact fit is obtained when the splitting due to the additional trigonal potential is equal to that produced by the twist.

Previous studies have reported a value of $0.6-0.7$ for k , while the parameters Δ and λ have not been varied independently. Rather the parameter $v = \Delta/\lambda$ has been found to have a value of about 3 and the ground state splitting assigned a value of $\sim 450 \text{ cm}^{-1}$ on the assumption that λ in the complex is only slightly reduced from the free ion value.

FIGURE 6.3

EFFECT ON AVERAGE MOMENT OF VARYING K

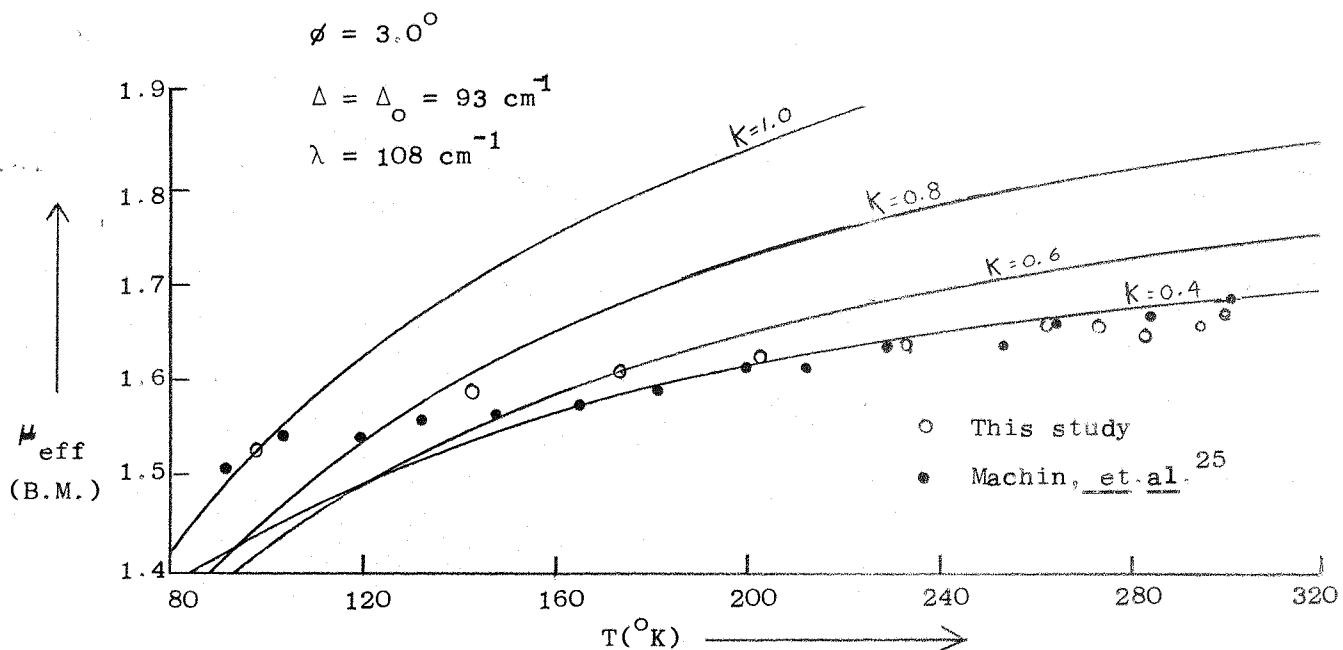


FIGURE 6.4

EFFECT ON AVERAGE MOMENT OF VARYING λ

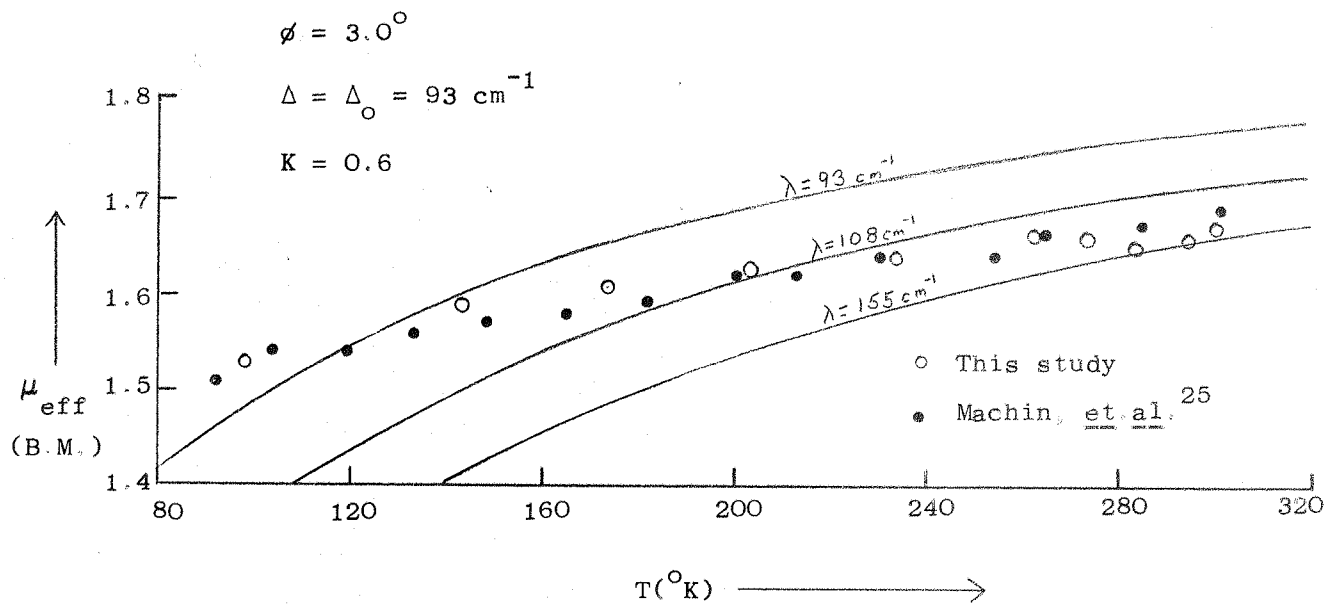


FIGURE 6.5

EFFECT ON AVERAGE MOMENT OF ADDITIONAL
SPLITTING OF GROUND STATE

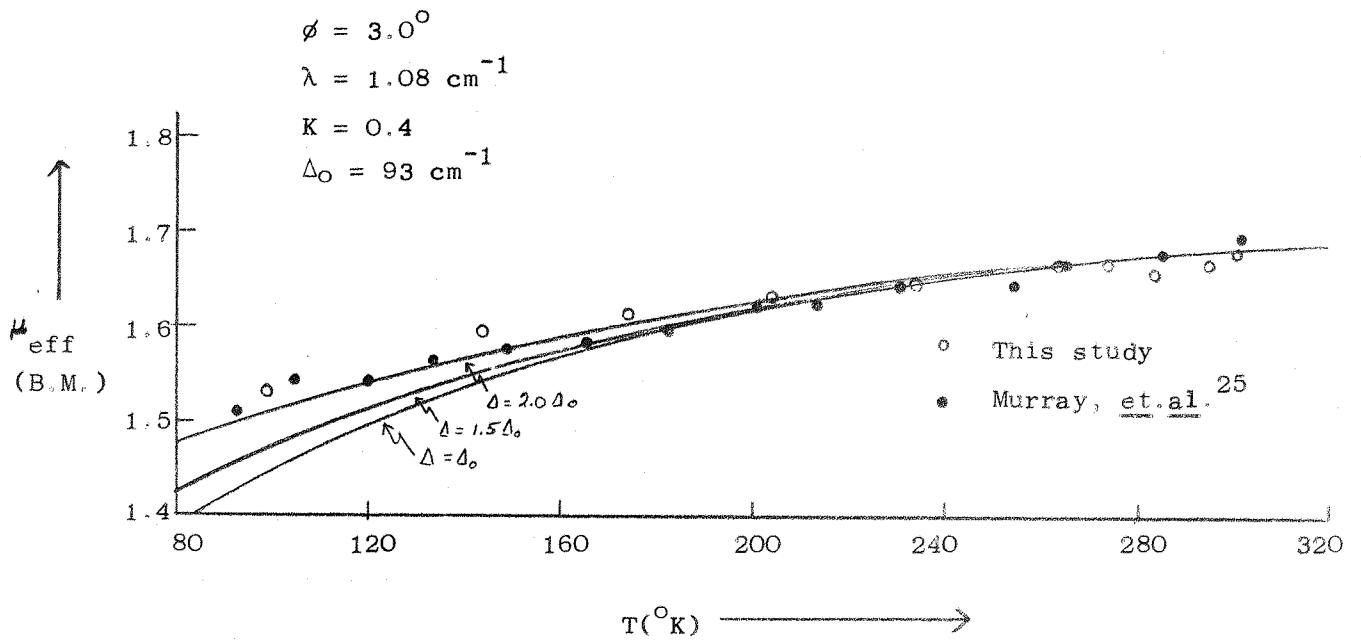


TABLE 6.1

MEASURED MAGNETIC MOMENTS

$T(^{\circ}\text{K})$	μ_{eff} (B.M.)
300	1.67
294	1.66
283	1.65
273	1.66
263	1.66
233	1.64
203	1.63
173	1.61
143	1.59
98	1.53

TABLE 6.2

MAGNETIC ANISOTROPIES

Parameters of best fit to experimentally determined average moments:

$$\varnothing = 3.0^\circ$$

$$\lambda = 108 \text{ cm}^{-1}$$

$$k = 0.4$$

$$\Delta = 2\Delta_o = 186 \text{ cm}^{-1}$$

Zero-order corrected energies (relative to 2A_1 at $-4Dq$ under the ligand field potential):

$$E_1(\varnothing_1, \varnothing_3) = -22.3 \text{ cm}^{-1}$$

$$E_2(\varnothing_2, \varnothing_4) = 262.7 \text{ cm}^{-1}$$

$$E_3(\varnothing_5, \varnothing_6) = 131.4 \text{ cm}^{-1}$$

CALCULATED MAGNETIC MOMENTS

$T(^{\circ}\text{K})$	$\mu_{\parallel} \text{ (B.M.)}$	$\mu_{\perp} \text{ (B.M.)}$	$\mu_{\parallel} \parallel \mu_{\perp} \text{ (B.M.)}$	$\bar{\mu} \text{ (B.M.)}$
320	1.698	1.694	0.004	1.695
300	1.691	1.685	0.006	1.687
280	1.684	1.675	0.009	1.678
260	1.676	1.663	0.013	1.667
240	1.667	1.649	0.018	1.655
220	1.657	1.634	0.023	1.641
200	1.645	1.615	0.030	1.625
180	1.633	1.594	0.038	1.607
160	1.619	1.569	0.050	1.586
140	1.603	1.540	0.063	1.562
120	1.586	1.508	0.078	1.535
100	1.568	1.473	0.095	1.505
80	1.548	1.438	0.110	1.475

That the value of λ in the complex should be less than the free-ion value is well documented. Intuitively it might seem that the ratio λ/λ_0 should be equal to K , for if the orbital angular momentum part of (2) were reduced by the same factor k as it is in the Zeeman operator, this would be equivalent to using a spin-orbit coupling constant $\lambda = k\lambda_0$. While it is reasonable that the ratio λ/λ_0 and the parameter k should be strongly correlated, there is no a priori reason for assuming that they should be equal. Moreover, as Gerloch⁵⁷ has pointed out, the reduction of L in the spin-orbit coupling operator could be expected to be less than its reduction in the Zeeman operator, since the former is determined in regions nearer the nucleus where the d-orbitals would be less likely to be influenced by electron delocalization effects. Theoretical considerations²⁹ serve to set a probable lower limit of 0.6-0.7 on the value of k in regular octahedral complexes. Much lower values of k are possible in tetrahedral or other complexes lacking a center of symmetry such that d-p mixing is possible.

The magnitude of the ligand field splitting of the ground state indicated by the parameters of the best fit to the magnetic data would seem to be physically realistic. The splitting due to the twist potential may be calculated exactly, and an approximate calculation of the splitting to be expected from the trigonal potential due to the iodide ions has indicated that it should be approximately equal in magnitude to that produced by the twist alone. Thus the low values of λ and k would also appear to be physically valid. The significance of the low value of k is difficult to assess. It may indicate that a significant amount of d-p mixing has taken place, or simply that there has been a large degree of electron

delocalization (which might be expected on the basis of the degree of electron delocalization in the free urea molecule).

(iv) Summary.

In conclusion, it has been possible to interpret the spectral and magnetic properties of Hexaureatitanium(III) iodide on the basis of a ligand field model derived from the x-ray structure determination. Consideration of the magnetic properties seems to indicate that second-nearest neighbor effects may be important.

In addition, a novel treatment of trigonally distorted molecules, which appears to have general applicability, has been developed.

CHAPTER 7

ATTEMPTED PREPARATION OF A COMPLEX OF TITANIUM(III) WITH THIOUREA

The subject of metal-sulfur bonding in transition metal complexes has received an increased amount of attention in the past several years. The first complexes of titanium(III) involving sulfur donor ligands have recently been reported,¹⁵ but, as yet, no ionic complexes involving a bond between titanium(III) and sulfur are known. Thiourea is known to form ionic complexes with a number of the transition metals. It was felt that if a complex of titanium(III) with thiourea could be prepared it would offer an interesting opportunity for comparing the coordinating behavior of oxygen and sulfur toward titanium(III).

It did not prove possible to prepare the desired complex in a manner analogous to that used in the case of the urea complex. Aqueous solutions of TiCl_3 and thiourea gave no visible evidence of the formation of a new complex, and, indeed, the absorption spectrum of such solutions throughout the region 800-350 $\text{m}\mu$ was identical to that of aqueous solutions of TiCl_3 alone. Cooling of a hot solution of TiCl_3 in water saturated with thiourea caused hair-like fibres of the ligand to precipitate. Pfeiffer⁵⁸ has prepared a hexaurea complex of chromium(III), but he formulates the complex with thiourea as $\text{CrCl}_3 \cdot 3\text{L}$. An attempt to adapt his procedure to the present case was unsuccessful. Evaporation to dryness in a nitrogen atmosphere of an aqueous solution of TiCl_3 and thiourea produced the following changes. Initially the color of the solution changed from red-violet to blue-black. Solutions of TiCl_3 in dilute aqueous HCl undergo a similar color change upon heating which Jørgensen⁵⁹ attributes

to the formation of mixed oxidation-state complexes in the solution. On further heating a yellow substance (possibly free sulfur) was deposited around the edges of the solution and a yellow-green crust began to form on the surface. The solution was now a dark red-brown color. (This color is also observed in the case of the chromium complex). The final residue remaining at dryness was yellow-green in color. Trituration with water through which nitrogen had been bubbled to remove dissolved oxygen produced an insoluble, lightly colored residue identified as TiO_2 .

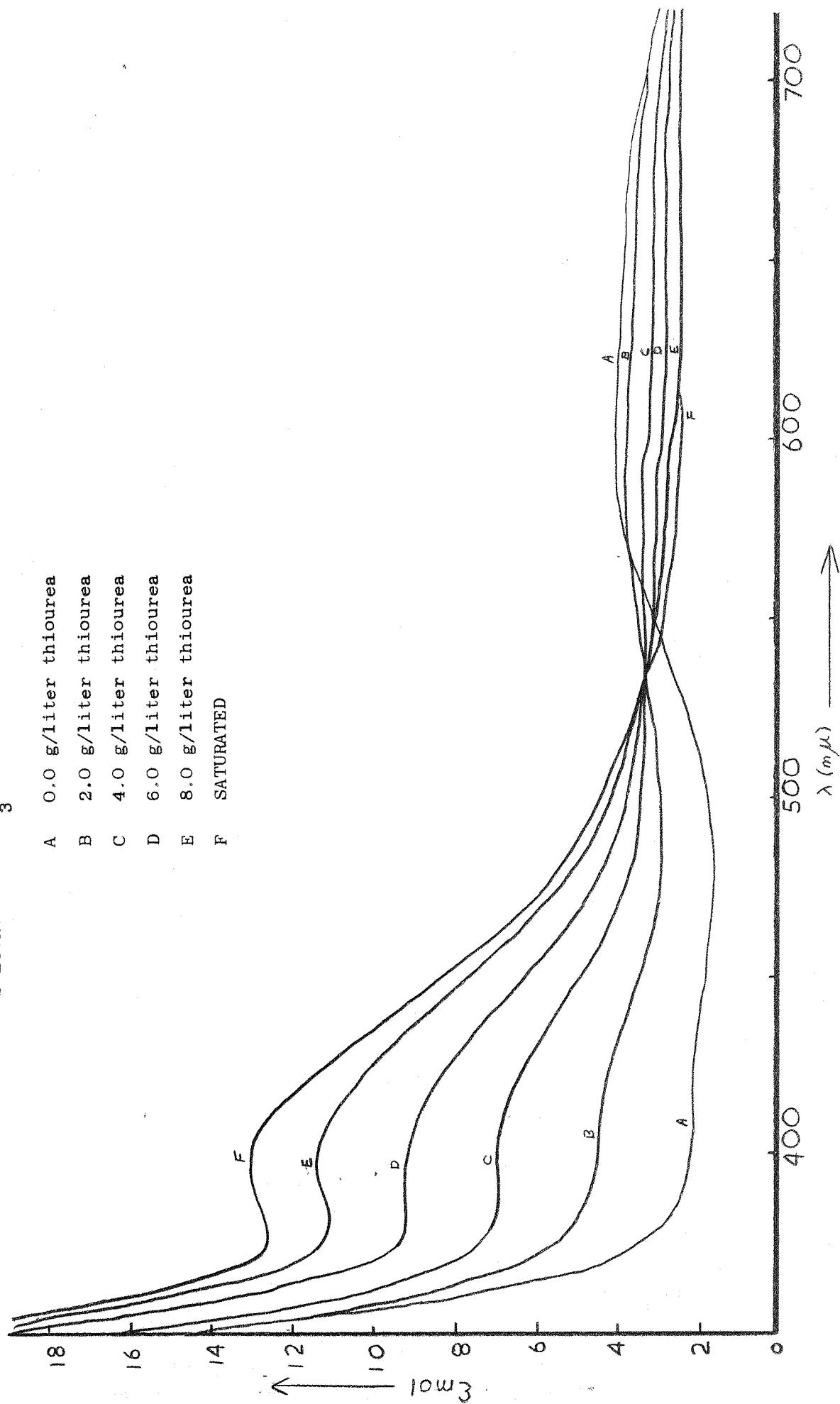
Several workers^{60,61} have reported that in aqueous solutions the N-monoalkyl derivatives of thiourea are stronger coordinating agents than thiourea itself, but attempts to prepare a complex with N-methylthiourea were similarly unsuccessful.

The preparation was next attempted using as the solvent various alcohols. These were chosen as being less strongly coordinating than water, but still capable of dissolving a moderate amount of thiourea. In contrast to the aqueous solutions, solutions of TiCl_3 and either thiourea or N-methylthiourea in methanol, ethanol, or i-propanol (only with heating) gave visible evidence of the formation of a new complex. While solutions of TiCl_3 alone in the alcohols are blue, addition of either thiourea or N-methylthiourea produces a color change to yellow-green or yellow depending on the quantity of ligand added.

The effect of adding varying amounts of thiourea to a solution of TiCl_3 in methanol was studied spectrophotometrically. The results are presented in Figure 7.1. The isosbestic point at $\sim 535 \text{ m}\mu$ indicates that only two species take part in the equilibrium and

FIGURE 7.1

SPECTRUM OF TiCl_3 IN METHANOL CONTAINING VARYING AMOUNTS OF THIOUREA



that the intermediate green coloration is due to a mixture of the blue alcoholic complex and the yellow thiourea containing complex. The exact nature of the thiourea containing complex is not evident from the spectra alone. To assign as a d-d transition the absorption at $\sim 400 \text{ m}\mu$ which characterises this complex would seem questionable. Such an assignment would require Dq for thiourea to be very much greater than for water, while previous studies⁶⁵~~66~~ have shown that the ligand field strengths of the two ligands are similar. Coming as it does on the edge of the intense charge transfer band at $\sim 300 \text{ m}\mu$, it is difficult to obtain an accurate estimate of the intensity of this characteristic absorption, but it would appear to be at least three times as great as that for the d-d transition in the alcoholic complex, rather greater than is normally observed for six-coordinate complexes of titanium(III). The double structure which seems to characterize the d-d bands of titanium(III) complexes is also not evident, although, again, it may be masked by the charge transfer band.

In spite of the evidence for the existence of a titanium(III)-thiourea complex in alcoholic solutions, it was not possible to isolate a solid complex corresponding to the yellow species. Concentration by gentle heating in a nitrogen of a solution on TiCl_3 and N-methylthiourea in methanol followed by evaporation to dryness in vacuo over P_2O_5 produced a dark violet solid which did not appear to be crystalline. A sample of this material was submitted to a commercial analysis for C, N, and H (Microanalytical Section, Department of Chemistry, University of Reading). The results of this limited analysis are compatible with the formulation $[\text{Ti}(\text{CH}_3\text{NHC:SNH}_2)_4(\text{CH}_3\text{OH})_2]\text{Cl}_3$.

Calculated for above formula--C:20.75%, N:19.36%; H:5.57%.

Found--C:20.52%, N:19.42%, H:5.53%.

It has not been possible to prepare this compound in a form suitable for an x-ray structure determination.

APPENDIX A

OBSERVED AND CALCULATED STRUCTURE FACTORS

		FO	FC	*h=2*	FO	FC	*h=1*	FO	FC	*h=7*	FO	FC	*h=10*	FO	FC
0	12	222.75	232.38	10	1 280.13	288.58	9	1 172.69	-172.79	0	4 171.45	-158.47	0	4 183.41	161.38
1	14	19.86	-18.34	10	4 112.88	-112.97	9	4 139.42	-145.04	1	0 50.60	-47.44	1	0 43.73	-39.07
2	10	167.45	-174.93	10	7 163.26	-163.26	9	7 141.73	148.00	1	3 131.09	124.27	1	3 89.18	-81.20
3	12	200.50	215.47	10	10 18.97	0.83	9	10 27.19	28.34	1	6 33.26	-22.62	1	6 86.97	-80.26
4	14	8.59	10.75	11	3 16.44	8.96	10	3 186.18	-181.30	1	9 27.00	-24.62	1	9 58.86	61.55
5	10	190.69	-192.72	11	6 123.44	-118.87	10	6 46.55	46.80	1	12 18.70	-9.04	2	2 91.08	92.41
6	12	94.74	89.39	11	9 18.97	7.10	10	9 79.24	79.70	2	2 209.60	233.43	2	5 213.72	224.33
8	10	181.94	-186.89	12	2 60.47	65.57	11	2 59.75	59.42	2	5 279.99	297.35	2	8 52.41	-53.98
9	12	54.67	51.93	12	5 116.48	128.10	11	5 52.64	-55.93	2	8 93.25	-92.13	2	11 80.31	-85.10
11	10	207.59	-211.55	12	8 31.35	30.17	11	8 23.67	-22.11	2	11 144.26	-146.42	3	1 102.91	-98.97
				13	1 117.20	123.57	12	1 112.92	-112.63	3	1 111.92	-114.49	3	4 86.47	85.19
				13	4 11.24	-2.57	12	4 24.12	-26.05	3	4 14.36	-1.11	3	7 77.81	-5.82
				13	7 128.82	-124.48	12	7 52.82	44.75	3	7 101.40	170.67	3	10 48.10	-42.95
				14	0 96.72	96.28	13	3 100.03	-107.48	3	10 23.26	-16.35	4	0 18.80	9.83
				14	3 29.14	42.85				4	3 151.79	-144.72	4	3 127.77	-116.77
				14	6 82.19	-83.89	*h=5*			4	6 121.63	172.27	4	6 35.64	28.29
				15	2 24.60	29.93	0	8 407.55	420.92	4	9 83.79	88.11	4	9 3.27	69.65
							0	14 78.14	-84.58	4	12 19.66	1.52	5	2 18.86	17.24
							1	1 245.12	267.49	5	2 33.10	35.47	5	5 139.11	139.43
							1	4 33.65	-17.98	5	5 198.48	164.68	5	8 19.25	7.57
							1	7 43.65	-161.31	5	8 87.98	-87.72	6	1 26.22	-20.11
							1	10 87.95	-44.16	5	11 72.57	-70.32	6	4 120.43	50.68
							1	13 61.01	61.12	6	1 164.72	-162.70	6	4 19.30	11.16
							2	0 14.09	2.39	6	4 19.72	9.53	7	0 81.68	-81.22
							2	3 178.50	-186.95	6	7 91.07	92.47	7	3 159.75	-157.47
							2	6 89.26	-82.02	6	10 19.10	-12.00	7	6 47.29	42.13
							2	9 124.99	124.95	7	0 131.53	-1	7	2 27.67	-26.77
							2	12 18.23	6.39	7	3 193.40	-194.70			
							3	2 319.76	-378.32	7	6 112.74	118.09			
							3	5 42.62	-40.05	7	9 108.18	139.22	0	2 323.89	-340.56
							3	8 296.52	-275.91	8	2 16.98	11.51	0	8 201.23	-197.92
							3	11 17.89	23.64	8	5 239.92	-242.72	1	1 102.39	-99.55
							3	1 273.89	294.73	8	10 50.35	-47.04	1	4 37.71	41.79
							4	4 154.02	-24.99	9	1 40.07	-42.43	1	7 53.39	52.05
							4	7 157.02	-154.03	9	4 18.09	-1.45	1	10 51.02	46.85
							4	10 17.25	5.59	9	7 19.18	13.56	2	0 181.70	189.31
							4	13 64.73	98.85	10	3 134.53	-134.08	2	3 53.45	50.34
							5	0 267.96	270.21	10	6 40.28	30.75	2	6 172.54	-169.06
							5	3 143.96	-146.85	11	2 22.64	-19.92	2	9 19.07	-21.49
							5	6 125.97	-116.98				3	2 215.02	-233.67
							5	9 44.86	47.12	*h=0*			3	5 17.66	10.73
							5	12 77.52	81.60				3	8 151.11	155.41
							5	12 280.78	-334.66	0	2 444.83	-517.15	3	4 120.44	-125.80
							6	2 280.78	98.33	0	8 375.17	384.99	4	4 58.60	-55.82
							6	5 97.89	98.33	1	1 52.64	54.77	4	7 69.12	63.11
							6	8 121.49	147.59	1	4 28.44	13.34	4	3 25.67	-21.08
							6	11 35.69	-33.35	1	7 33.80	-48.46	5	6 104.07	-167.09
							7	1 173.17	175.99	1	10 35.72	-32.83	5	2 27.22	-63.02
							7	4 46.26	-99.16	2	0 140.36	137.92	6	5 33.90	-38.59
							7	7 129.92	-125.41	2	3 33.35	-25.34	7	1 56.74	-28.91
							7	10 26.95	24.77	2	6 103.65	-97.29	7	4 8.50	8.30
							8	0 312.04	336.35	2	9 28.43	30.67			
							8	3 56.96	-55.42	2	12 51.04	49.48			
							8	6 171.21	-168.19	3	2 415.39	-488.96	*h=12*		
							8	9 18.50	7.18	3	5 15.49	-18.19	0	0 89.77	-91.59
							9	2 189.77	-115.51	3	8 260.32	241.89	0	6 24.07	-17.30
							9	5 61.48	62.59	3	11 19.06	0.30	1	2 64.46	70.64
							9	8 78.41	76.25	4	1 17.13	60.24	1	5 166.60	-175.94
							10	1 147.27	151.64	4	4 83.56	-73.37	1	8 59.99	-68.78
							10	4 17.57	-6.21	4	7 13.30	-70.71	2	1 161.09	158.34
							10	7 91.92	-92.42	4	10 7.49	-7.90	2	4 17.60	4.19
							11	0 172.55	199.59	5	3 15.91	2.59	2	7 98.82	-90.81
							11	3 24.24	-27.86	5	6 170.89	-160.77	3	0 58.99	-45.02
							11	6 169.12	-170.56	9	9 168.56	9.80	3	3 90.40	86.81
							12	2 31.25	-23.06	2	2 207.70	-223.46	6	4 48.55	43.45
							12	5 25.50	103.87	6	7 17.13	-23.06	7	2 73.08	71.91
							13	1 33.52	40.35	6	8 98.40	98.37	4	5 36.85	-33.57
										7	1 78.02	78.47	5	1 64.39	-60.66
							h=6			7	4 17.43	0.61	5	4 19.15	-15.99
							0	0 282.75	323.15	7	7 36.62	-35.83	6	0 71.14	-81.15
							0	6 261.92	-262.20	8	0 263.00	270.00	6	3 108.59	106.80
							0	12 67.04	68.07	8	3 45.83	19.13			
							1	2 297.80	332.16	8	6 197.09	-192.41	*h=13*		
							1	5 343.99	-370.94	9	2 57.18	-51.13	0	4 291.23	252.69
							1	8 15.97	-14.71	9	5 18.36	1.73	0	0 17.37	2.75
							1	11 141.97	139.31	10	1 37.48	40.94	1	3 80.99	-80.91
							2	2 25.67	-25.67	10	4 65.37	62.34	1	6 47.00	-36.61
							2	4 243.13	227.27				1	8 27.97	-25.53
							2	7 37.30	34.76	*h=9*			2	5 77.85	81.88
							2	10 155.93	-136.51	0	0 27.27	14.72	3	1 23.27	-4.52
							2	13 19.40	-23.70	0	6 68.82	-62.00	3	4 128.60	157.69
							3	0 136.29	144.70	0	12 8.48	-4.08	4	0 61.75	-55.34
							3	3 140.03	132.28	1	2 120.61	130.69	4	3 141.10	-144.22
							3	6 123.09	-118.39	1	5 275.52	-290.80	5	2 19.55	-14.31
							3	9 43.05	-43.55	1	8 60.35	-72.15			
							3	12 60.06	64.25	1	11 117.94	122.79	*h=11*		
							4	1 94.91	93.35	2	1 51.51	48.73	0	2 223.47	-229.14
							4	5 298.57	-301.09	2	4 112.29	104.40	1	8 86.63	-67.74
							4	8 90.48	-83.50	2	7 46.67	-46.34	1	1 107.14	-116.55
							4	11 100.38	105.55	2	10 40.00	-40.00	1	4 8.04	-3.02
							5	1 23.55	16.45	3	3 78.19	881.38	1	7 82.95	-80.88
							5	4 221.66	223.78	3	6 55.44	49.42	2	3 34.92	36.40
							5	7 24.07	17.97	3	9 66.89	-66.77	2	6 83.61	-77.30
							5	10 124.81	-123.97	4	2 57.20	60.01	3	2 64.54	-70.26
							6	3 169.46	169.93	4	5 138.99	-156.46	4	1 93.33	-98.06
							6	0 63.75	70.25	4	8 42.12	-36.97			
							6	6 61.07	48.90	5	1 59.11	48.82	*h=15*		
							6	122.97	-126.37	5	4 51.30	51.18	0	0 43.16	-41.47
							7	2 21.70	-46.65	5	7 89.39	-66.66	0	8 86.79	48.04
							7	5 113.09	-115.21	5	10 21.12	-48.20	1	2 20.94	3.33
							7	8 17.88	-19.21	6	3 206.99	207.43	2	1 139.70	135.23
							7	11 54.44	51.48	6	6 63.59	76.48			
							8								

Reflections marked by an * had an observed intensity equal to or less than the calculated standard deviation of the measurement. Such reflections were arbitrarily assigned an intensity equal to one half of the calculated standard deviation.

APPENDIX B

LEAST SQUARES WEIGHTING SCHEME FOR COUNTER COLLECTED

X-RAY DIFFRACTION INTENSITY DATA

In the application of the method of least squares (See Chap.2) there is associated with each measured value, F_i , of the variable a weight. This weight is a measure of the probable precision of the measured value and is properly equal to the reciprocal of the variance of that measurement

$$w_i = \frac{1}{\sigma_i^2} \quad (1)$$

where σ_i is the standard deviation in the i th observation.

It is possible to derive an expression for the probable standard deviation in counter measured x-ray diffraction intensities based on the statistics of counting. The x-ray pulses entering the counter may be characterized by a Poisson distribution and as such it can be shown that

$$\sigma_{\text{count}} = N^{\frac{1}{2}} \quad (2)$$

Both the peak count and the background count will be subject to such a statistical uncertainty. On this basis, the statistical uncertainty in the net intensity is given by⁶²

$$\sigma_I = (N_T + 0.25(t_c/t_b)^2(N_{B1} + N_{B2}))^{\frac{1}{2}} \quad (3)$$

where N_T is the total count obtained in a time t_c and N_{B1} and N_{B2} the background counts at each end of the scan range each obtained in a time t_b . If the time for which the background is counted is the same as that during which the peak is scanned (e.g. background

is counted for $\frac{1}{2}$ the scan time at each end of the scan range) this reduces to

$$\sigma_I' = (N_T + N_B)^{\frac{1}{2}} \quad (4)$$

To this expression for statistical fluctuations must be added a term to allow for random, non-statistical variations proportional to the net count (e.g. long term variations in beam intensity), resulting in a final expression of the form

$$\sigma_I = (N_T + N_B + (pN_N)^2)^{\frac{1}{2}} \quad (5)$$

Stout and Jensen³³ relate the parameter p to the standard deviation in the intensity of a reference reflection measured periodically throughout the data collection, assigning it a value of 0.01-0.02, but Corfield, Doedens, and Ibers⁶³ indicate that a larger value, of the order of 0.04-0.06, is necessary to avoid over-weighting very intense reflections.

From the relation between I and F_{rel} , it is possible to derive an expression for the standard deviation in F_{rel} , in terms of the standard deviation of I .

The basic relationship is

$$F = \sqrt{\frac{k}{L_p}} I \quad (6)$$

Where L_p is the Lorentz and polarization correction and k a scale factor. Differentiating (6) with respect to I

$$dF = \frac{1}{2} \sqrt{\frac{k}{L_p}} \frac{dI}{\sqrt{I}} \quad (7)$$

which may be re-expressed as

$$dF = \frac{1}{2}F \frac{dI}{I} \quad (8)$$

If (6) is solved for I and the result substituted into (8) and, in addition, the assumption made that for small deviations

$dF = \sigma_F$ and $dI = \sigma_I$, the final result is obtained that

$$\sigma_F = \frac{k}{2L_p F} \sigma_I \quad (9)$$

Thus, in view of equation (1), it can be seen that the proper weight to use in a least squares refinement based on F_{rel} is

$$w_{F_{rel}} = \frac{4L_p^2 F_{rel}^2}{k^2 \sigma_I^2} \quad (10)$$

where σ_I is given by equation (5).

APPENDIX C

ANISOTROPIC TEMPERATURE FACTOR RELATIONS FOR
ATOMS ON SPECIAL POSITIONS

Special constraints on the values of the anisotropic thermal parameters β_{ij} of atoms on special positions arise from the fact that the thermal ellipsoid of such an atom must conform to the point symmetry of the site. Levy⁶⁴ has shown that the β_{ij} transform under the symmetry operations of the space group as the quadratic products of the atomic coordinates and has used this fact as the basis of a method for determining the relations between thermal parameters of atoms related by symmetry operations and for determining the constraints on the thermal parameters of atoms in special positions. The essence of the method is embodied in two rules:

- (1) The β_{ij} for distinct positions are related as the quadratic products of the atomic coordinates, ignoring translational components, of the atoms related by the symmetry operation.
- (2) For the β_{ij} of atoms on special positions rule (1) holds, subject to the additional condition that the β_{ij} are invariant under any symmetry operation which leaves the position invariant.

In the case of the compound $[\text{Ti}(\text{CO}(\text{NH}_2)_2)_6]\text{I}_3$ which crystallizes in the space group $R\bar{3}c$ with the titanium atoms located on the special positions a (point symmetry $\bar{3}2$) and the iodide ions on the special positions e (point symmetry $\bar{1}$), the above rules may be applied as follows:

Titanium--Consider the symmetry operation of the space group which transforms the general position x, y, z into $-y, x-y, z$.

Application of this operation to the position $O,O,1/4$ leaves it unchanged.

$$\begin{array}{ll}
 \text{By rule (1) } q_1^* q_1^* = y^2 & \beta_{11}' = \beta_{22} \\
 q_2^* q_2^* = x^2 - 2xy + y^2 & \beta_{22}' = \beta_{11} - 2\beta_{12} + \beta_{22} \\
 q_3^* q_3^* = z^2 & \beta_{33}' = \beta_{33} \\
 q_1^* q_2^* = xy - y^2 & \beta_{12}' = \beta_{12} - \beta_{22} \\
 q_1^* q_3^* = yz & \beta_{13}' = \beta_{23} \\
 q_2^* q_3^* = xz - yz & \beta_{23}' = \beta_{13} - \beta_{23}
 \end{array}$$

But by rule (2), $\beta_{11}' = \beta_{11}$ $\beta_{23}' = \beta_{23}$. This restriction leads to two independent thermal parameters and the following relations:

$$\begin{array}{l}
 \beta_{11} = \beta_{22} = 2\beta_{12} \\
 \beta_{33} = \beta_{33} \\
 \beta_{13} = \beta_{23} = 0
 \end{array}$$

Iodide--Consider the symmetry operation which transforms x,y,z into $x-y,-y,1/2-z$ under which the position $x,O,1/4$ is invariant. Application of the rules in the manner shown above leads to four independent thermal parameters and the following relations:

$$\begin{array}{l}
 \beta_{11} = \beta_{11} \\
 \beta_{22} = 2\beta_{12} \\
 \beta_{33} = \beta_{33} \\
 \beta_{23} = 2\beta_{13}
 \end{array}$$

The subroutine PATCH below assigns the independent thermal parameters in accordance with the relations derived above and sets the dependent parameters to zero. The variables HHJ(1), HHJ(2),, HHJ(6) correspond to the thermal parameters $\beta_{11}, \beta_{22}, \dots, \beta_{23}$ respectively. The factor 2 has already been incorporated into the cross terms and so appears explicitly only in the expression relating two such terms. The first block of statements treat the thermal parameters for titanium, the second those for iodide, while statement (3) returns parameters for all other atoms to the main program unaltered.

The subroutine RESETEB assigns values to all six thermal parameters based on the relations derived above and the computed values of the independent parameters.

```

SUBROUTINE PATCH (IMSYM, I, TJ, HJ, HHJ, IREJKT, ATOM)
  DIMENSION HHJ(6)
  IF(1-9)3,2,1
1  HHJ(1)=HHJ(1)+HHJ(2)+HHJ(4)
  HHJ(2) = 0.0
  HHK(3)=HHJ(3)
  HHJ(4)=0.0
  HHJ(5)=0.0
  HHJ(6)=0.0
  GO TO 3
2  HHJ(1)=HHJ(1)
  HHJ(2)=HHJ(2)+HHJ(4)
  HHJ(3)=HHJ(3)
  HHJ(4)=0.0
  HHJ(5)=HHJ(5)+2.0*HHJ(6)
  HHJ(6)=0.0
3  RETURN
  END

```

```

SUBROUTINE RESETB(BETA, ATOM, NA)
  DIMENSION BETA(6)
  IF(ATOM-2HTI)1,2,1
1  IF(ATOM-3HI1-)3,4,3
2  BETA(2)=BETA(1)
  BETA(4)=0.5*BETA(1)
  GO TO 3
4  BETA(4)=0.5*BETA(2)
  BETA(6)=2.0*BETA(5)
3  RETURN
  END

```

APPENDIX D

SUMMARY OF MATRIX ELEMENTS USED IN MAGNETIC MOMENT CALCULATIONS

A. Complete spin-orbit coupling matrix and first-order corrected wave functions

ϕ_1	ϕ_3	ϕ_5	ϕ_2	ϕ_4	ϕ_6				
$a_1\alpha$	$a_1\beta$	$e^1\alpha$	$e^1\beta$	$e^2\alpha$	$e^2\beta$	$e^{*1}\alpha$	$e^{*1}\beta$	$e^{*2}\alpha$	$e^{*2}\beta$
O-E	0	0	β_1	0	0	0	β_2	0	0
0	O-E	0	0	β_1	0	0	0	β_2	0
0	0	$\alpha_1 + \Delta - E$	0	0	0	γ	0	0	λ
β_1	0	0	$-\alpha_1 + \Delta - E$	0	0	0	$-\gamma$	0	0
0	β_1	0	0	$\alpha_1 + \Delta - E$	0	0	0	$-\gamma$	0
0	0	0	0	0	$-\alpha_1 + \Delta - E$	$-\gamma$	0	0	γ
0	0	γ	0	0	$-\lambda$	$\alpha_2 - E$	0	0	0
β_2	0	0	$-\gamma$	0	0	0	$-\alpha_2 - E$	0	0
0	β_2	0	0	$-\gamma$	0	0	0	$\alpha_2 - E$	0
0	0	λ	0	0	γ	0	0	0	$-\alpha_2 - E$

$$\text{where } \alpha_1 = (c_1^2 - 2c_2^2)\lambda/2$$

$$\alpha_2 = (c_2^2 - 2c_1^2)\lambda/2$$

$$\beta_1 = (3/2)^{1/2}\lambda c_1$$

$$\beta_2 = (3/2)^{1/2}\lambda c_2$$

$$\gamma = 3c_1c_2\lambda/2$$

$\lambda = \lambda$ (spin-orbit coupling constant)

$\Delta = \Delta$ (splitting between a_1 and e^1 under the ligand field potential)

B. First-order corrected wave functions.

$$\begin{aligned} \phi_1 = & \sin\theta [|0, \frac{1}{2}\rangle - (3/2)^{\frac{1}{2}} c_2 \lambda / 10 D q (c_2 |1\rangle - c_1 |2\rangle, -\frac{1}{2})] - \\ & \cos\theta [(c_1 |1\rangle + c_2 |2\rangle, -\frac{1}{2}) + 3c_1 c_2 \lambda / 20 D q (c_2 |1\rangle - c_1 |2\rangle, -\frac{1}{2})] \end{aligned}$$

$$\begin{aligned} \phi_2 = & \cos\theta [|0, \frac{1}{2}\rangle - (3/2)^{\frac{1}{2}} c_2 \lambda / 10 D q (c_2 |1\rangle - c_1 |2\rangle, -\frac{1}{2})] + \sin\theta \\ & [(c_1 |1\rangle + c_2 |2\rangle, -\frac{1}{2}) + 3c_1 c_2 \lambda / 20 D q (c_2 |1\rangle - c_1 |2\rangle, -\frac{1}{2})] \end{aligned}$$

$$\begin{aligned} \phi_3 = & \sin\theta [|0, -\frac{1}{2}\rangle - (3/2)^{\frac{1}{2}} c_2 \lambda / 10 D q (c_2 |-1\rangle + c_1 |2\rangle, \frac{1}{2})] - \cos\theta \\ & [(c_1 |-1\rangle - c_2 |2\rangle, \frac{1}{2}) + 3c_1 c_2 \lambda / 20 D q (c_2 |-1\rangle + c_1 |2\rangle, \frac{1}{2})] \end{aligned}$$

$$\begin{aligned} \phi_4 = & \cos\theta [|0, -\frac{1}{2}\rangle - (3/2)^{\frac{1}{2}} c_2 \lambda / 10 D q (c_2 |-1\rangle + c_1 |2\rangle, \frac{1}{2})] + \sin\theta \\ & [(c_1 |-1\rangle - c_2 |2\rangle, \frac{1}{2}) + 3c_1 c_2 \lambda / 20 D q (c_2 |-1\rangle + c_1 |2\rangle, \frac{1}{2})] \end{aligned}$$

$$\begin{aligned} \phi_5 = & [c_1 |1\rangle + c_2 |2\rangle, \frac{1}{2}] - 3c_1 c_2 \lambda / 20 D q [c_2 |1\rangle - c_1 |2\rangle, \frac{1}{2}] - \\ & \lambda / 10 D q [c_2 |-1\rangle + c_1 |2\rangle, -\frac{1}{2}] \end{aligned}$$

$$\begin{aligned} \phi_6 = & [c_1 |-1\rangle - c_2 |2\rangle, -\frac{1}{2}] - 3c_1 c_2 \lambda / 20 D q [c_2 |-1\rangle + c_1 |2\rangle, -\frac{1}{2}] + \\ & \lambda / 10 D q [c_2 |1\rangle - c_1 |2\rangle, \frac{1}{2}] \end{aligned}$$

where $\tan 2\theta = 2\lambda c_1 (3/2)^{\frac{1}{2}} / [(c_1^2 - 2c_2^2)\lambda/2 - \Delta]$

C. Summary of non-zero matrix elements under the Zeeman operators

μ_{\parallel} and μ_{\perp} .

(i) μ_{\parallel} (omitting the factor β_H)

$$\langle \phi_1 | \phi_1 \rangle = - \langle \phi_2 | \phi_2 \rangle = k(c_1^2 - 2c_2^2)\cos^2\theta + (3/2)^{\frac{1}{2}} \frac{6kc_1^2c_2^2\lambda}{10Dq}$$

$$\sin\theta\cos\theta + \frac{9kc_1^2c_2^2\lambda}{10Dq} \cos^2\theta + \sin^2\theta - \cos^2\theta$$

$$\langle \phi_3 | \phi_3 \rangle = - \langle \phi_4 | \phi_4 \rangle = k(c_1^2 - 2c_2^2)\sin^2\theta - (3/2)^{\frac{1}{2}} \frac{6kc_1^2c_2^2\lambda}{10Dq}$$

$$\sin\theta\cos\theta - \frac{9kc_1^2c_2^2\lambda}{10Dq} \sin^2\theta - \sin^2\theta + \cos^2\theta$$

$$\langle \phi_5 | \phi_5 \rangle = - \langle \phi_6 | \phi_6 \rangle = k(c_1^2 - 2c_2^2) - \frac{9k\lambda c_1^2c_2^2}{10Dq} + 1$$

$$\langle \phi_5 | \phi_6 \rangle = \frac{6k\lambda c_1c_2}{10Dq}$$

$$\langle \phi_1 | \phi_2 \rangle = - \langle \phi_3 | \phi_4 \rangle = (3/2)^{\frac{1}{2}} \frac{3k\lambda c_1c_2^2}{10Dq} \cos^2\theta - (3/2)^{\frac{1}{2}}$$

$$\frac{3k\lambda c_1c_2^2}{10Dq} \sin^2\theta - k(c_1^2 - 2c_2^2)\sin\theta\cos\theta - \frac{9\lambda c_1^2c_2^2}{10Dq} \sin\theta\cos\theta$$

$$+ 2\sin\theta\cos\theta$$

(ii) (omitting the factor β_H)

$$\langle \phi_1 | \phi_3 \rangle = - \frac{3k\lambda c_2^2}{10Dq} \sin^2\theta - (3/2)^{\frac{1}{2}} 2kc_1\sin\theta\cos\theta - (3/2)^{\frac{1}{2}}$$

$$\frac{3kc_1c_2^2}{10Dq} \sin\theta\cos\theta + \sin^2\theta$$

$$\langle \phi_2 | \phi_4 \rangle = - \frac{3k\lambda c_2^2}{10Dq} \cos^2\theta + (3/2)^{\frac{1}{2}} 2kc_1\sin\theta\cos\theta + (3/2)^{\frac{1}{2}}$$

$$\frac{3kc_1c_2^2}{10Dq} \sin\theta\cos\theta + \cos^2\theta$$

$$\langle \phi_1 | \phi_4 \rangle = \langle \phi_2 | \phi_3 \rangle = (3/2)^{1/2} \frac{3}{2} \frac{kc_1^2 c_2^2 \lambda}{10Dq} (\sin^2 \theta - \cos^2 \theta) + (3/2)^{1/2}$$

$$c_1 k (\sin^2 \theta - \cos^2 \theta) - \frac{3kc_2^2 \lambda}{10Dq} \sin \theta \cos \theta + \sin \theta \cos \theta$$

$$\langle \phi_1 | \phi_5 \rangle = \langle \phi_3 | \phi_6 \rangle = (3/2)^{1/2} kc_1 \sin \theta - (3/2)^{1/2} \frac{kc_1 c_2^2 \lambda}{10Dq} \sin \theta +$$

$$\frac{k\lambda}{10Dq} \cos \theta - \cos \theta$$

$$\langle \phi_1 | \phi_6 \rangle = -\langle \phi_3 | \phi_5 \rangle = (3/2)^{1/2} \frac{2kc_2}{10Dq} \sin \theta + \frac{3kc_1 c_2 \lambda}{10Dq} \cos \theta$$

$$\langle \phi_2 | \phi_5 \rangle = \langle \phi_4 | \phi_6 \rangle = (3/2)^{1/2} kc_1 \cos \theta - (3/2)^{1/2} \frac{3}{2} \frac{kc_1 c_2^2 \lambda}{10Dq} \cos \theta -$$

$$\frac{k\lambda}{10Dq} \sin \theta + \sin \theta$$

$$\langle \phi_2 | \phi_6 \rangle = -\langle \phi_4 | \phi_5 \rangle = (3/2)^{1/2} \frac{2kc_2}{10Dq} \cos \theta - \frac{3kc_1 c_2 \lambda}{10Dq} \sin \theta$$

D. Expressions used in calculating* the principal magnetic moments.

$$\mu_{||}^2 = \left[\frac{3\langle \phi_1 | \phi_1 \rangle^2 - 6kT \langle \phi_2 | \phi_1 \rangle^2}{E_1 - E_2} \right] e^{-E_1/kT} + \left[\frac{3\langle \phi_2 | \phi_2 \rangle^2 - 6kT \langle \phi_2 | \phi_1 \rangle^2}{E_2 - E_1} \right] e^{-E_2/kT} \\ + 3[\langle \phi_5 | \phi_5 \rangle^2 + \langle \phi_5 - \phi_6 \rangle^2] e^{-E_3/kT} \\ \hline e^{-E_1/kT} + e^{-E_2/kT} + e^{-E_3/kT}$$

$$\mu_{\perp}^2 = 3\langle \phi_1 | \phi_3 \rangle^2 e^{-E_1/kT} + 3\langle \phi_2 | \phi_4 \rangle^2 e^{-E_2/kT} - 6kT \left[\frac{\langle \phi_1 | \phi_5 \rangle^2}{E_1 - E_2} + \right. \\ \left. \frac{\langle \phi_1 | \phi_5 \rangle^2 + \langle \phi_1 | \phi_6 \rangle^2}{E_1 - E_3} \right] e^{-E_1/kT} - 6kT \left[\frac{\langle \phi_1 | \phi_4 \rangle^2}{E_2 - E_1} + \right. \\ \left. \frac{\langle \phi_2 | \phi_5 \rangle^2 + \langle \phi_2 | \phi_6 \rangle^2}{E_2 - E_3} \right] e^{-E_2/kT} - 6kT \left[\frac{\langle \phi_1 | \phi_5 \rangle^2 + \langle \phi_1 | \phi_6 \rangle^2}{E_3 - E_1} + \right. \\ \left. \frac{\langle \phi_2 | \phi_6 \rangle^2 + \langle \phi_2 | \phi_5 \rangle^2}{E_3 - E_2} \right] e^{-E_3/kT} \\ \hline e^{-E_1/kT} + e^{-E_2/kT} + e^{-E_3/kT}$$

*

Since the energies associated with the above matrix elements appear in the formulae for the magnetic moments only as squares, elements which differ only in sign are computationally equivalent.

REFERENCES

1. H. Hartmann and H. L. Schlafer, Z. phys. Chem., 197 (1951), 116.
2. F. E. Ilse and H. Hartmann, Z. phys. Chem., 197 (1951), 239.
3. H. Hartmann, H. L. Schlafer and K. H. Hansen, Z. anorg. Chem., 284 (1956), 153.
4. H. Hartmann, H. L. Schlafer and K. H. Hansen, Z. anorg. Chem., 289, (1957), 40.
5. H. Lipson, Proc. Roy. Soc., A151 (1935), 347.
6. K. Spangenberg, Neues Jb. Mineral. Geol. Palaeontolog., Abt. A (1949), 99.
7. A. D. Liehr and C. J. Ballhausen, Ann. Phys., 3 (1958), 304.
8. A. Stahler, Ber., 37 (1904), 4405.
9. G. Brauer, Handbuch der präparativen anorganischen Chemie, Stuttgart (1954).
10. H. L. Schlafer and F. P. Fritz, Spectrochim. Acta, 23A (1967), 1409.
11. H. J. Gardner, Aust. J. Chem., 20 (1967), 2357.
12. A. Stahler, Ber., 38 (1905), 2619.
13. R. J. H. Clark, The Chemistry of Titanium and Vanadium, Elsevier, Amsterdam (1968).
14. H. L. Schlafer and R. Gotz, Z. anorg. Chem., 328 (1964), 1.
15. G. W. A. Fowles, T. E. Lester and R. A. Walton, J. Chem. Soc., A1968, 198.
16. G. A. Barbieri, Atti Reale Accad. Naz. Lincei, Rend., 24 (1915), 916.
17. R. J. H. Clark and M. L. Greenfield, unpublished work cited in 13.
18. C. M. O'Donnell and P. H. Davis, unpublished work.
19. M. Cox, Inorg. Synth., 9 (1967), 44.
- 20a. A. Linek, J. Siskova, and L. Jenšovský, Proc. 9th Intern. Conf. Coord. Chem., St. Moritz-Bad, Sept. 5-9, 1966.
- b. A. Linek, J. Siskova, and L. Jenšovský, Coll. Czech. Chem. Commun., 31 (1966), 4453.

21. J. H. Van Vleck, J. Chem. Phys., 7 (1939), 72.
22. R. Dingle, J. Chem. Phys., 50 (1969), 545.
23. J. Lewis, D. J. Machin, I. E. Newnham and R. S. Nyholm, J. Chem. Soc., 1962, 2036.
24. R. J. H. Clark, J. Lewis, D. J. Machin and R. S. Nyholm, J. Chem. Soc., 1963, 379.
25. D. J. Machin, K. S. Murray, and R. A. Walton, J. Chem. Soc., A1968, 195.
26. B. N. Figgis, Trans. Faraday Soc., 57 (1961), 198.
27. B. N. Figgis, J. Lewis, F. E. Mabbs, and G. A. Webb, Nature, 203 (1964), 1138.
28. B. N. Figgis, J. Lewis, F. E. Mabbs, and G. A. Webb, J. Chem. Soc., A1966, 422.
29. M. Gerloch and J. R. Miller, Progress in Inorg. Chem., 10 (1968), 1.
30. M. J. Bueger, X-Ray Crystallography, Wiley, New York (1942).
31. M. J. Bueger, Crystal Structure Analysis, Wiley, New York (1960).
32. E. W. Nuffield, X-Ray Diffraction Methods, Wiley, New York (1966).
33. G. H. Stout and L. H. Jensen, X-Ray Structure Determination, Macmillan, New York (1968).
34. A. L. Patterson, Z. Krist., A90 (1935), 517.
35. H. Bethe, Ann. Physik., 3 (1929), 133.
36. R. Schlapp and W. G. Penney, Phys. Rev., 41 (1932), 194.
37. R. Schlapp and W. G. Penney, Phys. Rev., 42 (1932), 666.
38. J. H. Van Vleck, J. Chem. Phys., 3 (1935), 803 and 807.
39. R. S. Mulliken, Phys. Rev., 41 (1932), 49.
40. R. S. Mulliken, Phys. Rev., 43 (1933), 279.
41. R. S. Mulliken, J. Chem. Phys., 3 (1935), 375.
42. J. H. Van Vleck, Electric and Magnetic Susceptibilities, Oxford University Press, Oxford (1932).
43. K. W. H. Stevens, Proc. Roy. Soc., A219 (1953), 542.
44. T. C. Furnas, Single Crystal Orienter Instruction Manual, General Electric Company, Milwaukee, (1957).

45. D. T. Cromer and J. T. Waber, Acta Cryst., 18 (1964), 8104.
46. R. F. Stewart, E. R. Davidson, and W. T. Simpson, J. Chem. Phys., 42 (1965), 3175.
- 47a. International Tables for X-Ray Crystallography, I (Symmetry Groups), N. F. M. Henry and K. Lonsdale eds., Kynoch Press, Birmingham, (1952).
- b. International Tables for X-Ray Crystallography, III (Physical and Chemical Tables), C. H. MacGillavry and G. D. Rieck eds., Kynoch Press, Birmingham (1962).
- 48a. J. DeMulenaer and H. Tompa, Acta Cryst., 19 (1965), 1014.
- b. J. DeMulenaer and H. Tompa, Union Carbide Research Associates (Brussels, Belgium), Technical Report 53/66.
49. W. R. Busing and H. A. Levy, Acta Cryst., 10 (1957), 180.
50. E. R. Andrew and D. Hyndman, Discuss. Faraday Soc., 19 (1955), 195.
51. J. E. Worsham, H. A. Levy, and S. W. Peterson, Acta Cryst., 10 (1957), 319.
52. A. Caron and J. Donohue, Acta Cryst., 17 (1964), 544.
53. C. J. Ballhausen, Introduction to Ligand Field Theory, McGraw-Hill, New York (1962).
54. B. N. Figgis, J. Chem. Soc., 1965, 4887.
55. A. D. Liehr and C. J. Ballhausen, Phys. Rev., 106 (1957), 1161.
56. M. Gerloch, J. Chem. Soc., A1968, 2023 (and references therein).
57. M. Gerloch and R. Slade, J. Chem. Soc., A1969, 1022.
58. P. Pfeiffer, Ber., 36 (1903), 1926.
59. C. K. Jørgensen, Acta Chem. Scand., 11 (1957), 73.
60. G. Yagupsky, R. H. Negrotti, and R. Levitus, J. Inorg. Nucl. Chem., 27 (1965), 2603.
61. T. J. Lane, J. W. Thompson, and J. A. Ryan, J. Am. Chem. Soc., 81 (1959), 3569.
62. W. R. Busing and H. A. Levy, J. Phys. Chem., 26 (1957), 563.
63. P. Corfield, R. Doedens, and J. Ibers, Inorg. Chem., 6 (1967), 197.
64. H. A. Levy, Acta Cryst., 9 (1956), 679.
65. O. Piovesana and C. Furlani, J. Inorg. Nucl. Chem., 30 (1968), 1249.